SCIENCE CHINA PRESS

SCIENCE CHINA Life Sciences
life.scichina.com link.springer.com
https://doi.org/10.1007/s11427-024-2704-7

RESEARCH PAPER

Versatile plant genome engineering using anti-CRISPR-Cas12a systems

Yao He[1,2†], Shishi Liu[2,3†], Long Chen[4,5†], Dongkai Pu[2], Zhaohui Zhong[2], Tang Xu[1], Qiurong Ren[2], Chuan Dong[2], Yawei Wang[2], Danning Wang[2], Xuelian Zheng[1], Fengbiao Guo[6,7*], Tao Zhang[4,5*], Yiping Qi[8,9*] & Yong Zhang[1,2*]

[1]Integrative Science Center of Germplasm Creation in Western China (Chongqing) Science City, Chongqing Key Laboratory of Tree Germplasm Innovation and Utilization, School of Life Sciences, Southwest University, Chongqing 400715, China;
[2]Department of Biotechnology, School of Life Sciences and Technology, Center for Informational Biology, University of Electronic Science and Technology of China, Chengdu 610054, China;
[3]Sichuan Institute of Edible Fungi, Sichuan Academy of Agricultural Sciences, Chengdu 610066, China;
[4]Jiangsu Key Laboratory of Crop Genomics and Molecular Breeding/Zhongshan Biological Breeding Laboratory/Key Laboratory of Plant Functional Genomics of the Ministry of Education, College of Agriculture, Yangzhou University, Yangzhou 225009, China;
[5]Jiangsu Co-Innovation Center for Modern Production Technology of Grain Crops/Jiangsu Key Laboratory of Crop Genetics and Physiology, Yangzhou University, Yangzhou 225009, China;
[6]Department of Respiratory and Critical Care Medicine, Zhongnan Hospital of Wuhan University, Wuhan 430017, China;
[7]Key Laboratory of Combinatorial Biosynthesis and Drug Discovery, Ministry of Education and School of Pharmaceutical Sciences, Wuhan University, Wuhan 430072, China;
[8]Department of Plant Science and Landscape Architecture, University of Maryland, College Park 20742, USA;
[9]Institute for Bioscience and Biotechnology Research, University of Maryland, Rockville 20850, USA

†Contributed equally to this work
*Corresponding authors (Yong Zhang, email: zhangyong916@swu.edu.cn; Yiping Qi, email: Yiping@umd.edu; Tao Zhang, email: zhangtao@yzu.edu.cn; Fengbiao Guo, email: fbguoy@whu.edu.cn)

Received 21 June 2024; Accepted 7 August 2024; Published online 15 August 2024

CRISPR-Cas12a genome engineering systems have been widely used in plant research and crop breeding. To date, the performance and use of anti-CRISPR-Cas12a systems have not been fully established in plants. Here, we conduct *in silico* analysis to identify putative anti-CRISPR systems for Cas12a. These putative anti-CRISPR proteins, along with known anti-CRISPR proteins, are assessed for their ability to inhibit Cas12a cleavage activity *in vivo* and *in planta*. Among all anti-CRISPR proteins tested, AcrVA1 shows robust inhibition of Mb2Cas12a and LbCas12a in *E. coli*. Further tests show that AcrVA1 inhibits LbCas12a mediated genome editing in rice protoplasts and stable transgenic lines. Impressively, co-expression of AcrVA1 mitigates off-target effects by CRISPR-LbCas12a, as revealed by whole genome sequencing. In addition, transgenic plants expressing AcrVA1 exhibit different levels of inhibition to LbCas12a mediated genome editing, representing a novel way of fine-tuning genome editing efficiency. By controlling temporal and spatial expression of AcrVA1, we show that inducible and tissue specific genome editing can be achieved in plants. Furthermore, we demonstrate that AcrVA1 also inhibits LbCas12a-based CRISPR activation (CRISPRa) and based on this principle we build logic gates to turn on and off target genes in plant cells. Together, we have established an efficient anti-CRISPR-Cas12a system in plants and demonstrate its versatile applications in mitigating off-target effects, fine-tuning genome editing efficiency, achieving spatial-temporal control of genome editing, and generating synthetic logic gates for controlling target gene expression in plant cells.

anti-CRISPR | Cas12a | AcrVA1 | off-target effects | fine-tuning genome editing | inducible and tissue specific genome editing | CRISPRa | synthetic logic circuit

INTRODUCTION

The CRISPR-Cas systems are acquired immune systems evolved by microorganisms to prevent invasion of bacteriophages and foreign genetic elements (Jinek et al., 2012). CRISPR-Cas systems are present in approximately 40% of bacteria and 90% of archaea (Grissa et al., 2007; Kunin et al., 2007). They can be broadly divided into two classes and six types. Class 1 systems (types I, III, and IV) have multi-protein effector complexes, while Class 2 systems (types II, V, and VI) use single protein effector molecules (Jinek et al., 2012; Makarova et al., 2020). The type II and type V systems are the most extensively studied and widely used systems for genome editing (Jinek et al., 2012; Makarova et al., 2020). Type II CRISPR-Cas systems are further categorized into subtypes (II-A, II-B, and II-C) based on the genetic arrangement of CRISPR loci and the sequence similarity of the Cas9 proteins (Makarova and Koonin, 2015; Makarova et al., 2020).

In order to fight bacterial CRISPR-Cas defense, bacteriophages have evolved small proteins that inactivate the CRISPR-Cas systems (Bondy-Denomy et al., 2013). In 2016, the first anti-CRISPR (Acr) of CRISPR-Cas9, AcrIIC1, was reported (Pawluk et al., 2016a). There are at least 44 type II Acr proteins identified (https://tinyurl.com/anti-CRISPR). Among these Acr proteins, AcrIIA5 and AcrIIA17 have been shown to exhibit multiple type II anti-CRISPR-Cas9 activity (Garcia et al., 2019; Hwang and Maxwell, 2023; Mahendra et al., 2020; Song et al., 2019), and AcrIIC1 has been shown to inhibit diverse type II-C Cas9 orthologs (Harrington et al., 2017). Research on these type II Acr proteins revealed different inhibitory mechanisms that target the loading of crRNA (Thavalingam et al., 2019; Wang et al., 2022; Zhu et al., 2019), the recognition and binding of target DNA/RNA (Dong et al., 2017; Liu et al., 2019; Shin et al., 2017; Yang

CrossMark click for updates

and Patel, 2017), and the cleavage of target nucleic acid (Liu et al., 2021; Sun et al., 2019). So far, type II Acrs have been widely explored for use as "off-switches" for CRISPR-Cas9 (Hwang and Maxwell, 2023). Type II-C Acrs, AcrIIC1 to AcrIIC5 have been successfully used to inhibit editing by NmeCas9 in human cells (Lee et al., 2018; Pawluk et al., 2016a), AcrIIC3 have been shown to repress CRISPR-dCas9 based transcriptional regulation (Nakamura et al., 2019), AcrIIC1 and AcriIC3 have been shown to control organ or cell type specific genome editing (Hoffmann et al., 2019; Lee et al., 2019a). Type II-A Acrs, AcrIIA2, AcrIIA4, and AcrIIA5, have been applied to reduce off-target editing in human cells (Liang et al., 2020; Nakamura et al., 2019). AcrIIA2 have been shown to inhibit gene drive (Basgall et al., 2018), AcrIIA1 and AcrIIA2 have been shown to repress CRISPR-dCas9 based transcriptional regulation (Nakamura et al., 2019). Furthermore, AcrIIA4 have been shown to inhibit gene drive (Basgall et al., 2018; D'Amato et al., 2024), repress CRISPR-dCas9 based transcriptional regulation (Nakamura et al., 2019), control organ or cell type specific genome editing (Hirosawa et al., 2019; Hoffmann et al., 2019; Mathony et al., 2020), mediate optical control of genome and epigenome editing (Bubeck et al., 2018). Recently, AcrIIA4 was shown to inhibit gene editing and activation mediated by the CRISPR-Cas9 system in *N. benthamiana* (Calvache et al., 2022). Also, AcrIIA4 and AcrIIA5 were used to inhibit base editing in Arabidopsis, *N. benthamiana*, and poplar cells (Liu et al., 2023). These plant cell-based assays demonstrated promising applications of anti-CRISPR systems in plant engineering and synthetic biology.

At present, five Acr, AcrVA1 to AcrVA5, have been identified to target CRISPR-Cas12a systems (Marino et al., 2018; Watters et al., 2018). AcrVA1 can bind to LbCas12a-crRNA complex to trigger the truncation of the crRNA, hence inhibiting LbCas12a-crRNA's ability to bind to target DNA (Knott et al., 2019b; Marino et al., 2018; Watters et al., 2018). AcrVA2 recognizes and binds to the N-terminus of Cas12a, triggering its mRNA disruption before translation is completed (Knott et al., 2019b; Zhang et al., 2019). AcrVA4 is a dimeric protein that forms the Cas12a-crRNA dimer, which subsequently inhibit DNA targeting by CRISPR-Cas12a (Knott et al., 2019a; Knott et al., 2019b; Peng et al., 2019; Zhang et al., 2019). AcrVA5 inhibits MbCas12a by acetylating the Lys635 residue required for PAM interactions. The acetylation of this site provides sufficient steric hindrance to block dsDNA binding and prevent cleavage (Dong et al., 2019). Although the mechanism of AcrVA3 for Cas12a inhibition is currently unclear, and studies have found that a homolog of AcrVA3, AcrVA3.1, has dual inhibitory activity on the type I-C and V-A CRISPR Cas systems (Marino et al., 2018).

Interestingly, most of the type V Acr proteins discovered so far inhibit more than one Cas12a orthologue (Dong et al., 2019; Knott et al., 2019a; Knott et al., 2019b; Marino et al., 2018; Peng et al., 2019; Watters et al., 2018; Zhang et al., 2019). It has been demonstrated that three type V-A Acrs (AcrVA1, AcrVA4, and AcrVA5) inhibit Cas12a in bacteria and human cells (Watters et al., 2018). AcrVA1 was used to mimic an OFF switch (NOT logic operation) inside a logic synthetic gene network in mammalian cells (Kempton et al., 2020). Testing of AcrVA1, AcrVA4, and AcrVA5 showed AcrVA4 significantly limited gene editing of LbCas12a in yeast (Yu and Marchisio, 2021). Recently, AcrVA1 was shown to inhibit Cas12a gene editing and regulation in *N. benthamiana* with a transient viral delivery system (Calvache et al., 2022). These results lay the foundation for the application of type V Acr proteins. However, further exploration is needed for the application of Acr proteins in eukaryotes, especially in plants.

In this study, we developed a computational and experimental pipeline for type V-A Acr proteins discovery and validation. Then, we established a versatile plasmid interference system in *E. coli* for rapidly characterizing Acrs. We evaluated the inhibitory effects of putative Acr proteins and known Acr proteins (Marino et al., 2018; Watters et al., 2018) using a versatile plasmid interference system in *E. coli* and a genome editing system in plants. Our analysis pinpointed AcrVA1 as the most robust Acr protein for the inhibition of two widely used Cas12a orthologs in plants, LbCas12a (He et al., 2024; Tang et al., 2018; Tang et al., 2017; Tang et al., 2019) and Mb2Cas12a (Hui et al., 2024; Zhang et al., 2021). Focusing on LbCas12a and AcrVA1 in rice, we showed in planta expression of AcrVA1 can effectively mitigate off-target effects and generate transgenic plants that are resistant to Cas12a genome editing. With inducible and tissue specific promoters, we demonstrated fine-tuned spaciotemporal control of genome editing. Finally, we built logic gates for sophisticated control of readouts in plant cells. Together, our work established a versatile system for the characterization of anti-CRISPR-Cas12a Acrs and their use for plant genetic engineering.

RESULTS

In vivo characterization of known and putative anti-CRISPR-Cas12a systems

To identify novel anti-CRISPR (Acr) genes, we developed a decision-tree-based model that incorporate five features (Figure 1A). Through this decision tree-based approach, we identified four potential Acr genes in *Lachnospiraceae bacterium* ND2006 (Table S1 in Supporting Information), and these genes are clustered together on the same strand, potentially forming an operon (Figure S1A in Supporting Information). Furthermore, Proksee (Grant et al., 2023) analysis of the genome revealed that these genes are in the vicinity of genomic hotspots, such as transfer and recombination of mobileOG categories (Table S2 in Supporting Information). We applied this Acr annotation strategy to another Cas12a-containing species, *Porphyromonas macacae* strain COT-192 OH2631, which identified two potential Acrs located within prophage segments in this species (Table S1 in Supporting Information). These genes in the genome are organized alongside adjacent proteins containing a helix-turn-helix (HTH) motif (Figure S1A in Supporting Information). The protein sequence length of these six genes falls within the typical range distribution of all identified anti-CRISPR proteins (Figure 1B). We further investigated the gene distribution by performing BLAST analysis on the six proteins against the NR database, revealing their phylum-specific distribution (Figure S1B in Supporting Information). The protein structures encoded by these genes, as predicted by RoseTTAFold, display a significant enrichment in helix and loop structures (Figure S1B in Supporting Information). It is noteworthy that AcrVA1, AcrVA4 and AcrVA5 exhibited different types of high concentration of helix and loop regions (Figure S2A and B in Supporting Information), suggesting these previously characterized Acr proteins inhibit Cas12a through various mechanisms (Marino, 2023) that may be different from those of the candidate Acr

https://doi.org/10.1007/s11427-024-2704-7

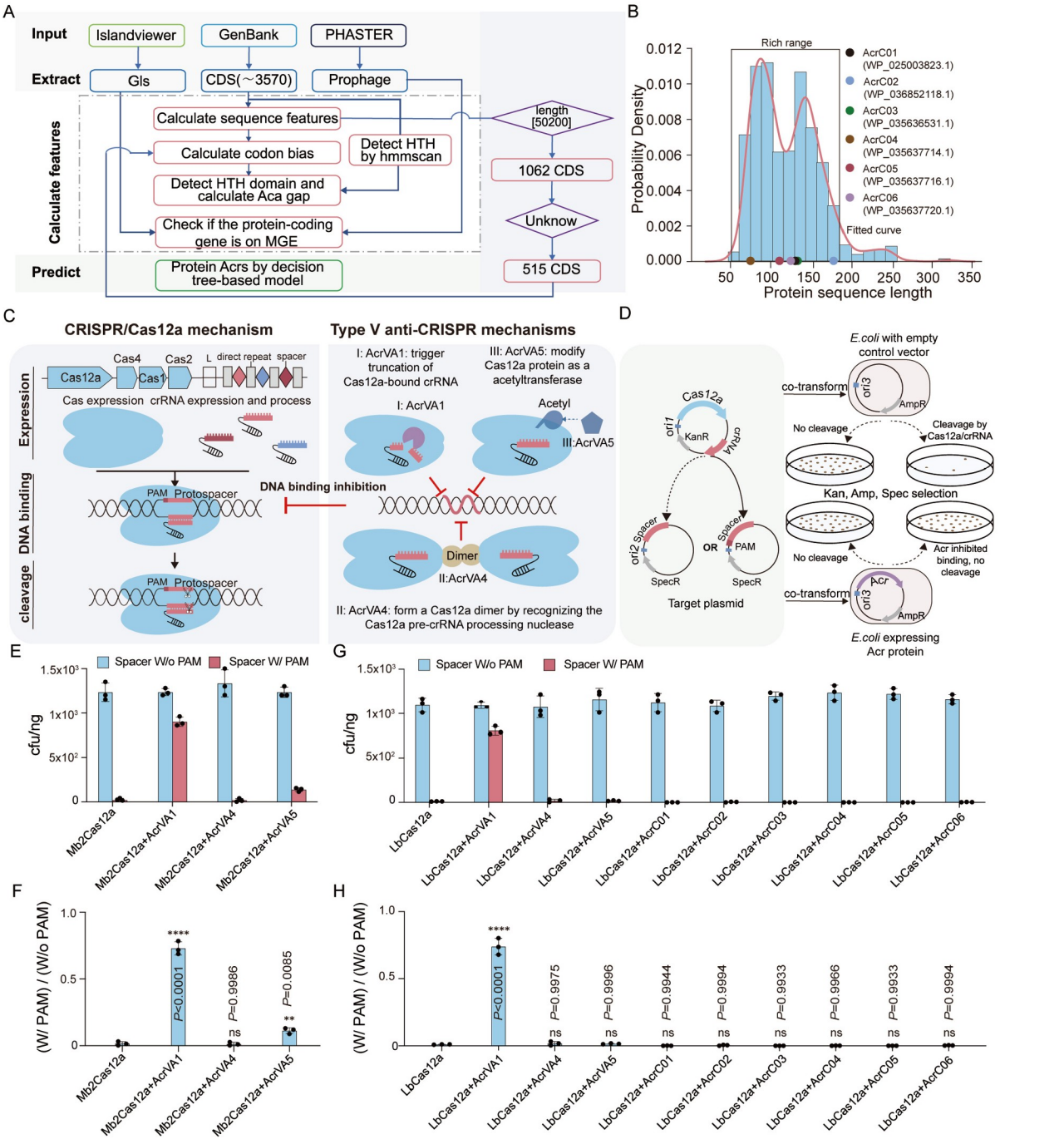

Figure 1. *In vivo* characterization of multiple anti-CRISPR-Cas12a systems. A, The pipeline employed for identifying potential anti-CRISPRs. B, The protein length distribution of the six potential anti-CRISPRs. C, Stages of CRISPR-Cas12a mechanism and type V-A anti-CRISPR mechanisms. Left panel: the stages of CRISPR-Cas12a mechanism. In the expression stage, the CRISPR array is transcribed into pre-crRNA, then the Cas12a proteins express by Cas genes processed it into single crRNA (violet, light red, and crimson,) that act as guides for Cas nucleases (blue). In the interference stage, the Cas12a nuclease guided by crRNA finds cognate sequences and binds to target binding sites. In the cleavage stage, the target DNA is cleaved and degraded. Right panel: the mechanisms of type V-A anti-CRISPR. AcrVA1, AcrVA4, and AcrVA5 exert inhibitory functions by inhibiting the binding of Cas-crRNA complexes to DNA. AcrVA1 (purple) cleaves Cas12a's crRNA, AcrVA4 (yellow) form a Cas12a dimmer. AcrVA5 (Dark Blue) inhibits Cas12a via post translational acetylation (Ac). D, Schematic overview of designed plasmids and procedure of plasmid interference assays for anti-CRISPR activity analysis in *E. coli*. AmpR, ampicillin resistance; KanR, kanamycin resistance; SpecR, spectinomycin resistance. E-H, The results of above plasmid interference assays. E, The bar plot of colony forming units (cfu) of each anti-CRISPR against Mb2Cas12a in *E. coli*. Each dot represents a biological replicate. Each target contains three biologicals. F, Bar graphs show the calculated inhibitory activity of each anti-CRISPR against Mb2Cas12a in *E. coli*. Inhibitory activity of each anti-CRISPR was shown in percentage by calculating the ratio of cfu between *E. coli* transformed with Cas12a plasmid with PAM+ matching spacer and that of the only matching spacer. Each dot represents a biological replicate. Each target contains three biological replicates. Error bars represent the mean values±SD (ns, $P>0.05$; ****, $P<0.0001$, one-way ANOVA, Dunnett's test). G, The bar plot of cell units of each anti-CRISPR against LbCas12a in *E. coli*. Each dot represents a biological replicate. Each target contains three biologicals. H, Bar graphs show the calculated inhibitory activity of each anti-CRISPR against LbCas12a in *E. coli*, Inhibitory activity of each anti-CRISPR was shown in percentage by calculating the ratio of cfu between *E. coli* transformed with Cas12a plasmid with PAM+ matching spacer and that of the only matching spacer. Each dot represents a biological replicate. Each target contains three biological replicates. Error bars represent the mean values±SD (ns, $P>0.05$; ****, $P<0.0001$, one-way ANOVA, Dunnett's test).

proteins identified here (Figure 1C and Figure S2C in Supporting Information).

Plasmid interference assays have been successfully adopted in screening type II-A and II-C Acrs against diverse CRISPR-Cas9 systems (Bondy-Denomy et al., 2013; Forsberg et al., 2019; Rauch et al., 2017; Song et al., 2023; Song et al., 2022; Uribe et al., 2019) and screening AcrVA5 against MbCas12a (Dong et al., 2019). To assess the cleavage activity of Mb2Cas12a and LbCas12a in bacteria, we first employed a depletion assay based on a double-antibiotics selection system in *E. coli* (Zhong et al., 2023) (Figure S3 in Supporting Information). To investigate the inhibitory activity of putative type V-A Acr proteins, we first developed a plasmid interference system in *E. coli* by using compatible bacterial plasmids harboring an exogenous CRISPR-Cas12a system, an exogenous type V-A Acr (AcrVA), and a target spacer with or without PAM sequence (Figure 1D). The inhibitory activity of each Acr can be measured by calculating the cfu (colony forming units) and the cfu ratio between *E. coli* transformed with Cas12a+spacer containing PAM and *E. coli* transformed with Cas12a+spacer without PAM. We chose Mb2Cas12a, which is efficient Cas12a (Hui et al., 2024; Zhang et al., 2021) and highly homologous to MbCas12a whose strain contains the AcrVA, and LbCas12a, which is widely used in eukaryotes (Liang et al., 2023; Ren et al., 2023; Tang et al., 2017; Tang et al., 2019; Zetsche et al., 2015; Zhong et al., 2018; Zhou et al., 2023). For Mb2Cas12a, we found AcrVA1 showed most pronounced inhibition effect, followed by AcrVA5, while AcrVA4 barely exhibited any inhibitory activity in *E. coli* (Figure 1E and F). For LbCas12a, we compared the six putative Acr proteins with AcrVA1, 4 and 5. Consistent with Mb2Cas12a, LbCas12a was strongly inhibited by AcrVA1; however, AcrVA5 failed to show inhibition activity in *E. coli* (Figure 1G and H), which was consistent with the previously reported *in vitro* data and the data in mammalian cells (Marino et al., 2018; Watters et al., 2018). Overall, our plasmid interference assays in *E. coli* identified AcrVA1 as a potent anti-CRISPR protein for both Mb2Cas12a and LbCas12a, and AcrVA5 as a mild anti-CRISPR protein for Mb2Cas12a, not for LbCas12a. The absence of inhibitory effects on LbCas12a by the six putative Acr proteins suggest they are either pseudo Acr proteins or their potential inhibitory activity is beyond the detection limit in this bacterial assay.

In planta characterization of select anti-CRISPR systems for inhibition of Cas12a-mediated genome editing

To further compare these Acr proteins, we next examined their abilities to block LbCas12a-mediated gene editing in plants, using rice as our test platform. We designed two types of all-in-one vectors, the first containing Cas12a expression unit and crRNA expression unit, and the second containing Cas12a expression unit, crRNA expression unit, and Acr expression unit. We selected the *OsPDS*-cR01 site with high editing activity by LbCas12a as previously shown in rice (Tang et al., 2018; Tang et al., 2017). First, we compared these Acr proteins in rice protoplasts (Figure 2A). The editing efficiency of LbCas12a was 64.4%; when AcrVA1 was co-expressed, the editing efficiency of LbCas12a was 0.25%, which was close to the detection limit of amplicon sequencing (Figure 2B). By contrast, co-expression of AcrVA4, AcrVA5, AcrC01, AcrC02, AcrC03, AcrC04, AcrC05, or AcrC06 did not exhibit any inhibitory effects (Figure 2B). To further verify that the significant decrease in editing efficiency was due to co-expression of AcrVA1, not due to co-expression of any other protein, we tested four endogenous rice loci using all-in-one vectors co-expressing LbCas12a, crRNA, and eYFP. The data from all four target sites showed that co-expression of eYFP did not reduce genome editing efficiency, suggesting the observed reduction of genome editing efficiency by AcrVA1 was indeed AcrVA1 specific (Figure S4 in Supporting Information).

We also conducted rice stable transformation to compare genome editing efficiency at the *OsPDS*-cR01 locus when an Acr protein was co-expressed (Figure 2C). When LbCas12a was expressed alone, 61.1% editing efficiency and 44.4% biallelic editing efficiency were observed. When AcrVA1 was co-expressed, the mutation efficiency and biallelic editing efficiency was reduced to 5.3% and 0.0%, respectively, indicating significant inhibition of LbCas12a genome editing by AcrVA1 in rice. Among the other eight Acr proteins tested, AcrVA4 and AcrC03 also significantly reduced genome editing efficiency, with 35.0% and 23.1% editing efficiencies, respectively (Figure 2D). Interestingly, such inhibitory effects by AcrVA4 and AcrC03 were not observed in the bacterial plasmid interference assay (Figure 1G and H) and the rice protoplast assay (Figure 2B), suggesting that stable transformation of plants is a more sensitive system for the detection of potential inhibitory effects of Acr proteins (Figure 2D).

Next, we used multiplexed editing to further compare AcrVA1, AcrVA4, AcrVA5, and AcrC03 for inhibition effects of LbCas12a in rice protoplasts. Very strong inhibition of LbCas12a by AcrVA1 was observed at all four target sites (Figure 2E). AcrVA4 showed significant inhibition at three out of four target sites: *OsGW2*-cR01, *OsCirc25329*-cR01, and *OsMPK21*-cR01 (Figure 2E). AcrVA5 only showed slight reduction of LbCas12a editing at one target site (*OsGW2*-cR01), while AcrC03 failed to reduce editing efficiency at all four sites (Figure 2E). However, none of the Acr proteins could alter the editing profiles of LbCas12a (Figure S5 in Supporting Information), suggesting they do not change the mode of action of LbCas12a. To confirm these observations, we conducted stable rice transformation using these same constructs except AcrC03. Analysis of T_0 lines showed that LbCas12a resulted in 63.6%, 59.1%, 77.3%, and 86.4% editing efficiency at the four target sites, respectively. After co-expression of AcrVA1, the editing efficiency was significantly reduced to 15.8%, 5.3%, 5.3%, and 5.3%, respectively (Figure 2F). After co-expression of AcrVA4 or AcrVA5, the editing efficiency of all four loci was also decreased, but to a less extent (Figure 2F). These data suggest that AcrVA1 is a very potent anti-LbCas12a protein, with much stronger inhibitory effects than AcrVA4 and AcrVA5 in rice protoplasts and stable lines.

To investigate generality of the above observation, we also tested the effects of AcrVA1, AcrVA4, AcrVA5, and AcrC03 on Mb2Cas12a with multiplexed editing at the same four target sites in rice. As with LbCas12a, Mb2Cas12a's genome editing activity was greatly inhibited by AcrVA1 (Figure 2G). However, none of the other three Acr proteins showed inhibitory effects on Mb2Cas12a in rice protoplasts (Figure 2G). Furthermore, while AcrVA1 could inhibit Mb2Cas12a, it did not change genome editing profiles (Figure S6 in Supporting Information). We then tested these systems using rice stable transformation. In stable rice lines, Mb2Cas12a generated 65.0%, 60.0%, 75.0%, and 75.0% genome editing efficiency at the four target sites, respectively (Figure 2H), very similar to the LbCas12a system (Figure 2F). Among 20 independent T_0 lines, no single edit could

https://doi.org/10.1007/s11427-024-2704-7

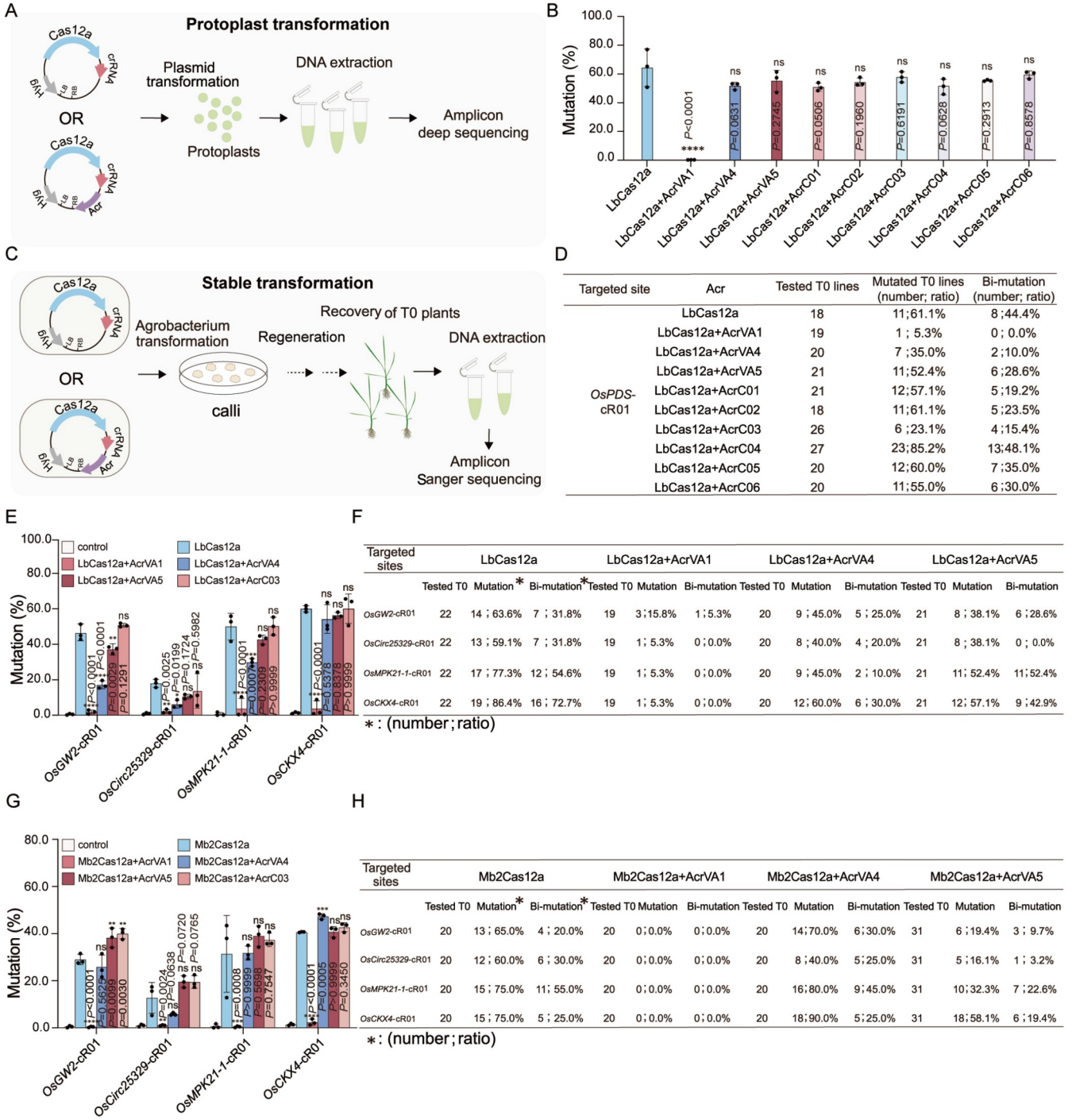

Targeted site	Acr	Tested T0 lines	Mutated T0 lines (number; ratio)	Bi-mutation (number; ratio)
OsPDS-cR01	LbCas12a	18	11;61.1%	8;44.4%
	LbCas12a+AcrVA1	19	1 ; 5.3%	0 ; 0.0%
	LbCas12a+AcrVA4	20	7 ;35.0%	2 ;10.0%
	LbCas12a+AcrVA5	21	11;52.4%	6 ;28.6%
	LbCas12a+AcrC01	21	12;57.1%	5 ;19.2%
	LbCas12a+AcrC02	18	11;61.1%	5 ;23.5%
	LbCas12a+AcrC03	26	6 ;23.1%	4 ;15.4%
	LbCas12a+AcrC04	27	23;85.2%	13;48.1%
	LbCas12a+AcrC05	20	12;60.0%	7 ;35.0%
	LbCas12a+AcrC06	20	11;55.0%	6 ;30.0%

Targeted sites	LbCas12a			LbCas12a+AcrVA1			LbCas12a+AcrVA4			LbCas12a+AcrVA5		
	Tested T0	Mutation*	Bi-mutation*	Tested T0	Mutation	Bi-mutation	Tested T0	Mutation	Bi-mutation	Tested T0	Mutation	Bi-mutation
OsGW2-cR01	22	14 ; 63.6%	7 ; 31.8%	19	3;15.8%	1 ;5.3%	20	9 ; 45.0%	5 ; 25.0%	21	8 ; 38.1%	6 ;28.6%
OsCirc25329-cR01	22	13 ; 59.1%	7 ; 31.8%	19	1; 5.3%	0 ;0.0%	20	8 ; 40.0%	4 ; 20.0%	21	8 ; 38.1%	0 ; 0.0%
OsMPK21-1-cR01	22	17 ; 77.3%	12 ; 54.6%	19	1; 5.3%	0 ;0.0%	20	9 ; 45.0%	2 ; 10.0%	21	11; 52.4%	11;52.4%
OsCKX4-cR01	22	19 ; 86.4%	16 ; 72.7%	19	1; 5.3%	0 ;0.0%	20	12; 60.0%	6 ;30.0%	21	12; 57.1%	9 ;42.9%

*: (number ; ratio)

Targeted sites	Mb2Cas12a			Mb2Cas12a+AcrVA1			Mb2Cas12a+AcrVA4			Mb2Cas12a+AcrVA5		
	Tested T0	Mutation*	Bi-mutation*	Tested T0	Mutation	Bi-mutation	Tested T0	Mutation	Bi-mutation	Tested T0	Mutation	Bi-mutation
OsGW2-cR01	20	13 ; 65.0%	4 ; 20.0%	20	0;0.0%	0;0.0%	20	14;70.0%	6;30.0%	31	6 ;19.4%	3 ; 9.7%
OsCirc25329-cR01	20	12 ; 60.0%	6 ; 30.0%	20	0;0.0%	0;0.0%	20	8 ;40.0%	5;25.0%	31	5 ;16.1%	1 ; 3.2%
OsMPK21-1-cR01	20	15 ; 75.0%	11; 55.0%	20	0;0.0%	0;0.0%	20	16;80.0%	9;45.0%	31	10;32.3%	7 ;22.6%
OsCKX4-cR01	20	15 ; 75.0%	5 ; 25.0%	20	0;0.0%	0;0.0%	20	18;90.0%	5;25.0%	31	18;58.1%	6 ;19.4%

*: (number ; ratio)

Figure 2. Efficient in planta inhibition of LbCas12a and Mb2Cas12a genome editing by anti-CRISPR systems. A, Editing activity evaluation workflow of Cas12a nucleases without anti-CRISPR or with anti-CRISPR in rice protoplasts. See details in Methods. The all-in-one plasmid harbors cassettes expressing Cas12a, crRNA or/and anti-CRISPR. B, Editing efficiency of protoplasts transformed with LbCas12a nucleases without anti-CRISPR or with nine different anti-CRISPR in *OsPDS*-cR01 site. Editing efficiency was quantified by NGS of PCR amplicons. Each dot represents a biological replicate. Each target contains three biological replicates. Error bars represent the mean values±SD (ns, $P>0.05$; ****, $P<0.0001$, Ordinary one-way ANOVA, Dunnett's test). C, Editing activity evaluation workflow of Cas12a nucleases without anti-CRISPR or with anti-CRISPR in rice through Agrobacterium-mediated transformation. The all-in-one plasmid harbors cassettes expressing Cas12a, crRNA or/and anti-CRISPR. D, The mutant rates of LbCas12a nucleases without anti-CRISPR or with nine different anti-CRISPR in *OsPDS*-cR01 site in rice T_0 lines. E, Editing efficiency of protoplasts transformed with LbCas12a nucleases without anti-CRISPR or with four different anti-CRISPR in four sites (multiplex editing, include *OsGW2*-cR01, *OsCirc25329*-cR01, *OsMPK21-1*-cR01, *OsCKX4*-cR01). Editing efficiency was quantified by NGS of PCR amplicons. Each dot represents a biological replicate. Each target contains three biological replicates. Error bars represent the mean values ±SD (ns, $P>0.05$; *, $P<0.05$; **, $P<0.01$; ***, $P<0.001$; ****, $P<0.0001$, Ordinary one-way ANOVA, Dunnett's test). F, The mutant rates of LbCas12a nucleases without anti-CRISPR or with three different anti-CRISPR in four sites in rice T_0 lines. G, Editing efficiency of protoplasts transformed with Mb2Cas12a nucleases without anti-CRISPR or with four different anti-CRISPR in four sites. Editing efficiency was quantified by NGS of PCR amplicons. Each dot represents a biological replicate. Each target contains three biological replicates. Error bars represent the mean values±SD (ns, $P>0.05$; *, $P<0.05$; **, $P<0.01$; ***, $P<0.001$; ****, $P<0.0001$, one-way ANOVA, Dunnett's test). H, The mutant rates of Mb2Cas12a nucleases without anti-CRISPR or with three different anti-CRISPR in four sites in rice T_0 lines.

be detected at all four target sites when AcrVA1 was co-expressed (Figure 2H). Significant reduction of genome editing efficiency was observed with AcrVA5, not with AcrVA4, at all four target sites (Figure 2H). These in planta data is consistent with the bacterial plasmid interference assay (Figure 1E and F). Taken together, our data suggest strong *in planta* inhibition of LbCas12a and Mb2Cas12a by AcrVA1, mild inhibition of LbCas12a and Mb2Cas12a by AcrVA5. While AcrVA4 to some extent could inhibit LbCas12a in transgenic plants, they failed to exhibit such effects on Mb2Cas12a. Since AcrVA1 has excellent performance in inhibiting both Cas12a nucleases, we decided to focus on AcrVA1 to demonstrate its innovation applications in plants.

Reduced off-target effects of LbCas12a in rice by anti-CRISPR effector AcrVA1

Previous studies have shown that type II Acrs such as AcrIIA2, AcrIIA4, and AcrIIA5 can reduce the off-target effects of Cas9 in animal cells (Garcia et al., 2019; Liang et al., 2020; Rauch et al., 2017). To test whether type V-A Acr can reduce off-target effects of Cas12a genome editing in plants, we selected a total of 19 T_0 plants for whole genome sequencing (WGS), including four lines edited by LbCas12a, six lines edited by LbCas12a+AcrVA1, and five lines edited by LbCas12a+AcrVA5, along with control plants (Figure 3A and B). Sequencing reads of all plants were mapped to the rice genome (Table S3 in Supporting Information) to reveal the mutations identified in different plant groups (Figure 3C). The number of all insertions and deletions (InDels) observed in *Agrobacterium* only (Agro only: plants regenerated from *Agrobacterium*-mediated transformation of a control vector without the LbCas12a system) control plants ranged from 71 to 96, attributed to somatic clonal variation induced by tissue culture. The number of all InDels in LbCas12a ranged from 106 to 115, indicating off-target occurrence within the genome (Figure 3D). The number of all InDels in LbCas12a+AcrVA1 ranged from 85 to 96, similar to the control plants (Figure 3D), indicating a great reduction of genome-wide off-target effects of LbCas12a by AcrVA1. The number of all InDels in LbCas12a+AcrVA5 ranged from 93 to 106, showing slight reduction off-target mutations in the rice genome (Figure 3D). These mutations appeared to be present in all genomic regions across the genome, especially in intergenic and repeat region (Figure 3E). The number of SNVs observed in the Agro only control plants ranged from 99 to 129 (Figure 3F), indicating SNV somatic clonal variation induced by tissue culture. The number of SNVs in LbCas12a plants ranged from 171 to 233, indicating off-target occurrence within the genome; The number of SNVs in LbCas12a+AcrVA1 ranged from 115 to 159, and the number of SNVs in LbCas12a+AcrVA5 ranged from 142 to 157, indicating reduced off-target mutations by AcrVA1 and AcrVA5 (Figure 3F). These mutations appeared to be present in all genomic regions across the genome (Figure 3G). Further analysis showed that C:G>T:A and C:G>A:T mutations were predominant mutation types (Figure S7A in Supporting Information). Analysis of the allele frequencies of InDels and SNVs among T_0 lines showed similar patterns among transgenic T_0 lines, revealing mostly somaclonal variation features (Figure S7B and C in Supporting Information).

We also used the Cas-OFFinder (Bae et al., 2014) to predict potential off target sites dependent on crRNAs. With WGS data, we analyzed top off-target sites with mismatches $\leqslant$ 5 of four target sites (Figure 3H and Figure S7D in Supporting Information). Off-target mutations were detected in three such off-target sites in LbCas12a edited plants (Figure 3H). However, only one off-target site was edited in LbCas12a-edited lines when AcrVA1 or AcrVA5 was expressed (Figure 3H). Together, our results demonstrated that AcrVA1 and AcrVA5 can mitigate off-target effects of LbCas12a in rice.

Fine-tuning of LbCas12a genome editing in rice via constitutive expression of AcrVA1

Based on AcrVA1's strong effects of inhibiting on-target and off-target editing, we explored an idea of using AcrVA1 to fine-tune genome editing by LbCas12a. We took a sequential transformation approach (Figure 4A). We first obtained stable transformed rice plants expressing AcrVA1 with *nptII* resistance gene and screening with G418. After qPCR analysis, plants with different levels of AcrVA1 expression are propagated to obtain seeds (Figure 4A and B). Subsequently, these transgenic plants were transformed with the CRISPR-LbCas12a multiplexed genome editing construct based hygromycin resistance gene and screening with hygromycin (Figure 4A). Mutation analysis was conducted on the CRISPR-LbCas12a plants after secondary transformation. We found that in the plants that do not express AcrVA1, the mutation efficiency of the four loci was 73.9%, 60.9%, 82.6%,100% and the efficiency of biallelic mutation was 43.4%, 21.7%, 39.1%, 56.5%, respectively; In plants with low expression of AcrVA1, the mutation efficiency at four loci was 57.1%, 35.7%, 50.0%, 42.9% and the efficiency of biallelic mutation was 14.3%, 14.3%, 7.1%, 21.4%, respectively, indicating a decrease in editing efficiency; In plants with high expression of AcrVA1, the mutation efficiency at four loci was 10.0%, 0.0%, 6.67%, 13.3% and the efficiency of biallelic mutation was 0.0%, 0.0%, 0.0%, 3.3%, respectively, indicating a significant decrease in editing efficiency and biallelic mutation efficiency (Figure 4C). Thus, these results suggest we can use transgenic AcrVA1 plants to fine-tune CRISPR-Cas12a genome editing efficiency. Based on our off-target analysis, tuning down genome editing efficiency would help enhance targeting specificity in the plant genome. Furthermore, the over 7-fold reduction of genome editing efficiency observed in AcrVA1 high expression lines suggest that it is possible to engineer AcrVA1 expression plants that are largely resistant to Cas12a-mediated genome editing (Figure 4D).

Spaciotemporal control of LbCas12a genome editing in rice by inducible and tissue-specific expression of AcrVA1

To further explore tunability of LbCas12a-mediated genome editing, we wanted to test inducible and tissue specific promoters to drive AcrVA1 expression. Toward this end, we designed two AcrVA1 expression patterns, one by an estrogen-inducible promoter (e.g. XVE promoter) (Tang et al., 2016; Zhang et al., 2010; Zuo et al., 2000) (Figure 5A) and the other by a root-specific promoter (e.g., *OsRCc3* promoter) (Jeong et al., 2013; Yan et al., 2020) (Figure 5E). The expression box for the chimeric estrogen receptor protein activator (XVE) is located downstream of the terminator of the AcrVA1 expression cassette (not shown). Estrogen inducible expression of AcrVA1, coupled with constitutive expression of the CRISPR-LbCas12a system, would help achieve chemical inducible genome editing in plant cells (Figure 5B). We test the systems in rice protoplasts. In the absence of

https://doi.org/10.1007/s11427-024-2704-7

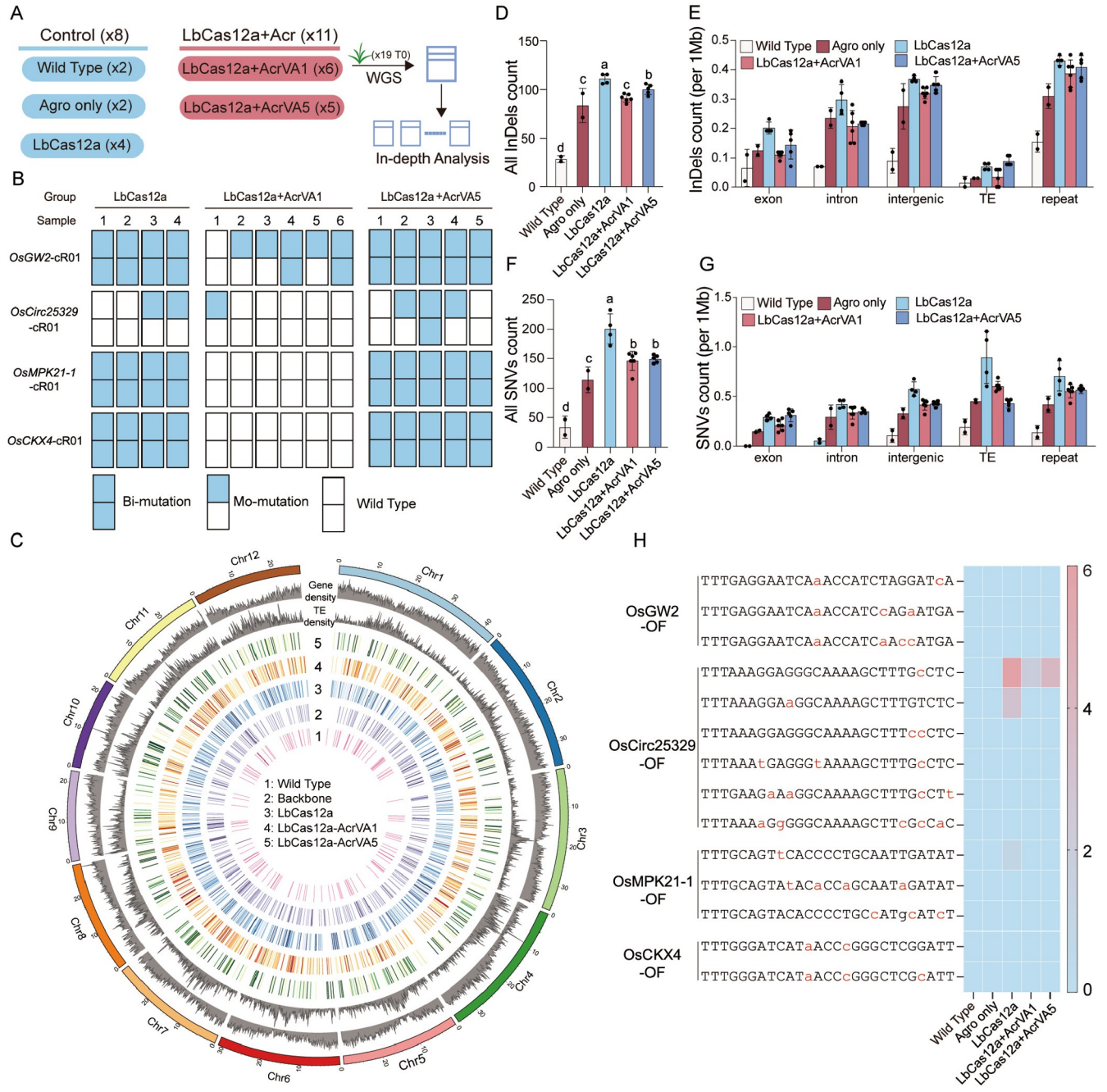

Figure 3. Minimizing off-target effects of LbCas12a by AcrVA1 in rice by whole-genome sequencing. A, Three groups of controls are included for assessing different background mutations. B, Multiple T_0 lines edited by different Acr-included editor constructs are chosen for assessing off-targeting by WGS. C, Genome-wide distribution of SNVs in all sequenced samples. D, Number of InDels mutations in all sequenced samples. Each dot represents a biological replicate. Each target contains two to six biological replicates. Different small letters indicate significant differences (P<0.05; one-way analysis of variance, LSD post hoc test). E, Average number of InDels mutations in per 1 Mbp genomic region. F, Number of single nucleotide variation (SNV) mutations in all sequenced samples. Each dot represents a biological replicate. Each target contains two to six biological replicates. Different small letters indicate significant differences (P<0.05; one-way analysis of variance, LSD post hoc test). G, Average number of SNV mutations in per 1 Mbp genomic region. H, Genome-wide landscape analysis of part gRNA-dependent off-target mutations.

AcrVA1 in the construct, the editing efficiency of LbCas12a at four target sites is 33.8%, 14.4%, 45.3%, and 50.7%; when AcrVA1 is constitutively expressed, the editing efficiency of the four targeted sites is 0.51%, 3.71%, 1.91%, and 0.34% (Figure 5C). As expected, AcrVA1 significantly reduced the editing efficiency of LbCas12a. However, without the addition of β-estradiol, the pXVE::AcrVA1 CRISPR-LbCas12a generated substantially lower editing efficiency than the CRISPR-LbCas12a construct at the four targeted sites: 8.7%, 8.6%, 22.0%, and 29.4%, indicating a leaky expression of the XVE promoter (Tang et al., 2016). When β-estradiol was added, the editing efficiency of the pXVE::AcrVA1 CRISPR-LbCas12a construct at four targeted sites was significantly reduced: 0.73%, 3.97%, 2.18%, and 1.95%, similar to the level when AcrVA1 was constitutively

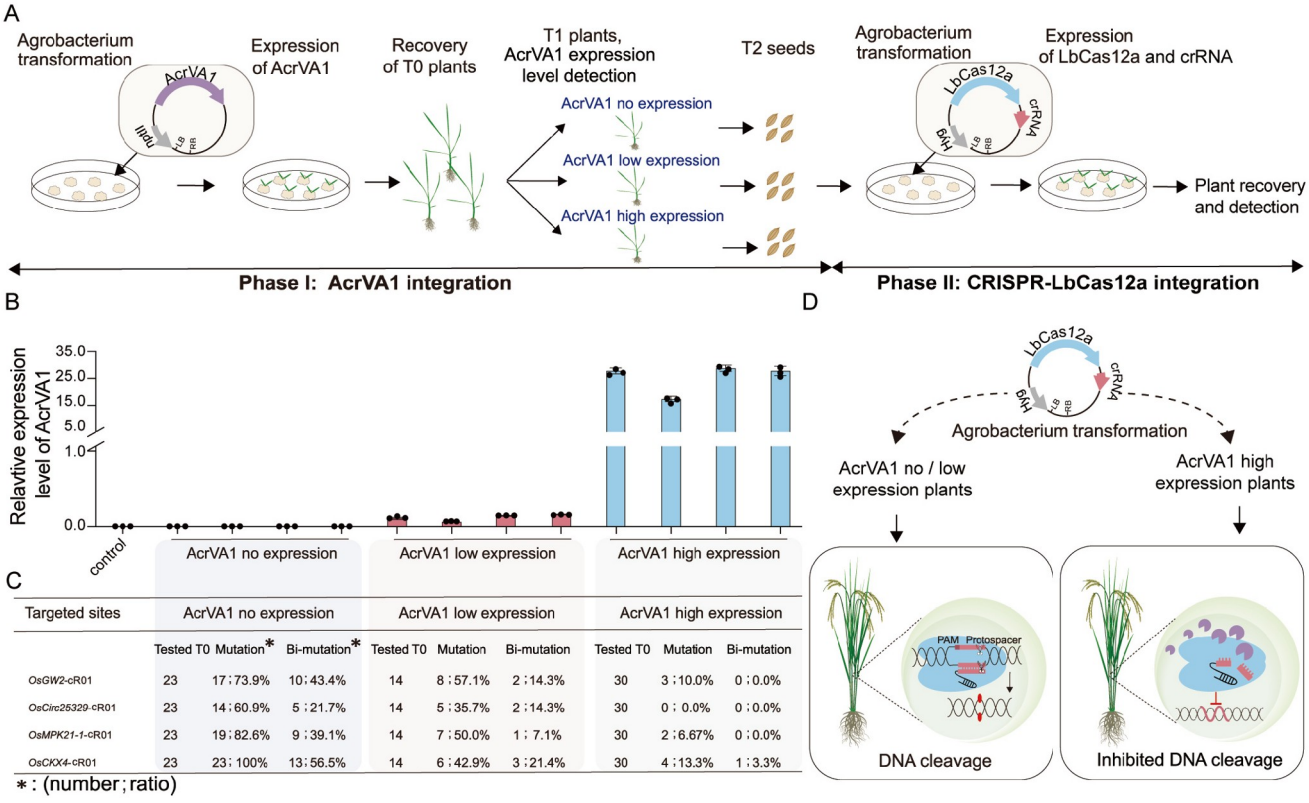

Targeted sites	AcrVA1 no expression			AcrVA1 low expression			AcrVA1 high expression		
	Tested T0	Mutation*	Bi-mutation*	Tested T0	Mutation	Bi-mutation	Tested T0	Mutation	Bi-mutation
OsGW2-cR01	23	17 : 73.9%	10 : 43.4%	14	8 : 57.1%	2 : 14.3%	30	3 : 10.0%	0 : 0.0%
OsCirc26329-cR01	23	14 : 60.9%	5 : 21.7%	14	5 : 35.7%	2 : 14.3%	30	0 : 0.0%	0 : 0.0%
OsMPK21-1-cR01	23	19 : 82.6%	9 : 39.1%	14	7 : 50.0%	1 : 7.1%	30	2 : 6.67%	0 : 0.0%
OsCKX4-cR01	23	23 : 100%	13 : 56.5%	14	6 : 42.9%	3 : 21.4%	30	4 : 13.3%	1 : 3.3%

*: (number : ratio)

Figure 4. AcrVA1-expressing plants are resistant to Cas12a genome editing. A, Schematic overview of sequential transformation. B, Relative expression level of AcrVA1 in 12 T_1 transgenic plants. C, The mutant rates of LbCas12a nucleases without anti-CRISPR or with the different AcrVA1 expression level in four sites in rice. D, Potential applications of AcrVA1-expressing plants in tunable genome engineering.

expressed (Figure 5C). We next evaluated the effectiveness of inducible expression of AcrVA1 in stable transgenic plants, using the same multiplexed CRISPR-LbCas12a construct. As a control, the LbCas12a construct generated high genome editing efficiency at four target sites (ranging from 59.1% to 86.4%); when AcrVA1 was expressed by the strong pZmUbi1 promoter, the genome editing efficiency was drastically reduced at all four target sites (ranging from 5.3% to 15.8%) (Figure 5D). When pXVE::AcrVA1 was present in the constructs, slight reduction of genome editing efficiency was observed at the four target sites (ranging from 16.7% to 55.6%), indicating leakiness of the XVE promoter (Figure 5D). Strong reduction of genome editing (ranging from 10.0% to 35.0%) occurred when β-estradiol was added in the tissue culture medium (Figure 5D), indicating inducible repression of genome editing effects. Together, our data from rice protoplasts and stable transgenic plants demonstrate efficient control of LbCas12a genome editing by using a chemical inducible promoter to drive AcrVA1 expression.

To demonstrate tissue-specific genome editing, we used a root-specific promoter, pOsRCc3 (Jeong et al., 2013; Yan et al., 2020), to drive AcrVA1 expression. Based on this design, we expected to see great reduction of genome editing in root cells, but not in the aboveground tissue (Figure 5F). We compared this construct (Figure 5E) with LbCas12a and LbCas12a+pZmUbi1::AcrVA1 in rice protoplasts. Impressively, we did not see any reduction of genome editing efficiency at the four target sites in leaf cells, when AcrVA1 was expressed by the root-specific promoter; By contrast, significant reduction of genome editing in root cells was observed (Figure 5G). Hence, our data suggest tissue-specific depletion of genome editing can be achieved by tissue-specific expression of an Acr protein such as AcrVA1.

Construction of logic gates with CRISPRa and anti-CRISPR systems in plant cells

The T-rich PAM requirement of Cas12a has also made it an efficient transcriptional regulatory tool, for targeting A-T rich promoter regions (Campa et al., 2019; Griffith et al., 2023; He et al., 2024; Tang et al., 2018; Tang and Zhang, 2023; Zhou et al., 2023). To evaluate the effect of AcrVA1 on LbCas12a-based transcriptional activation, we generated CRISPRa systems with and without the co-expression of AcrVA1 (Figure 6A). One targeted site per gene was designed in the promoter regions of four independent endogenous genes in rice: *OsER1*, *OsGW7*, *OsWaxy*, and *OsMIR528*. It is noteworthy that our CRISPRa system has achieved robust transcriptional activation (3.9 to 9.7-fold) of all four genes, based on the rice protoplast assay (Figure 6B). Strikingly, none of the four genes was transcriptional activated by CRISPRa when AcrVA1 was co-expressed (Figure 6B), suggesting strong inhibition of dLbCas12a mediated CRISPRa by AcrVA1.

Encouraged by the above data, we set to engineer programmable logic circuitry in plant cells by sophisticated control of CRISPRa and the corresponding anti-CRISPR system. We implemented five logic gate components in our system, which included a cassette expressing two fluorescent reporters: eYFP and mCherry (A1 cassette), a cassette expressing mCherry while the eYFP is driven by a minimal promoter that can be activated

https://doi.org/10.1007/s11427-024-2704-7

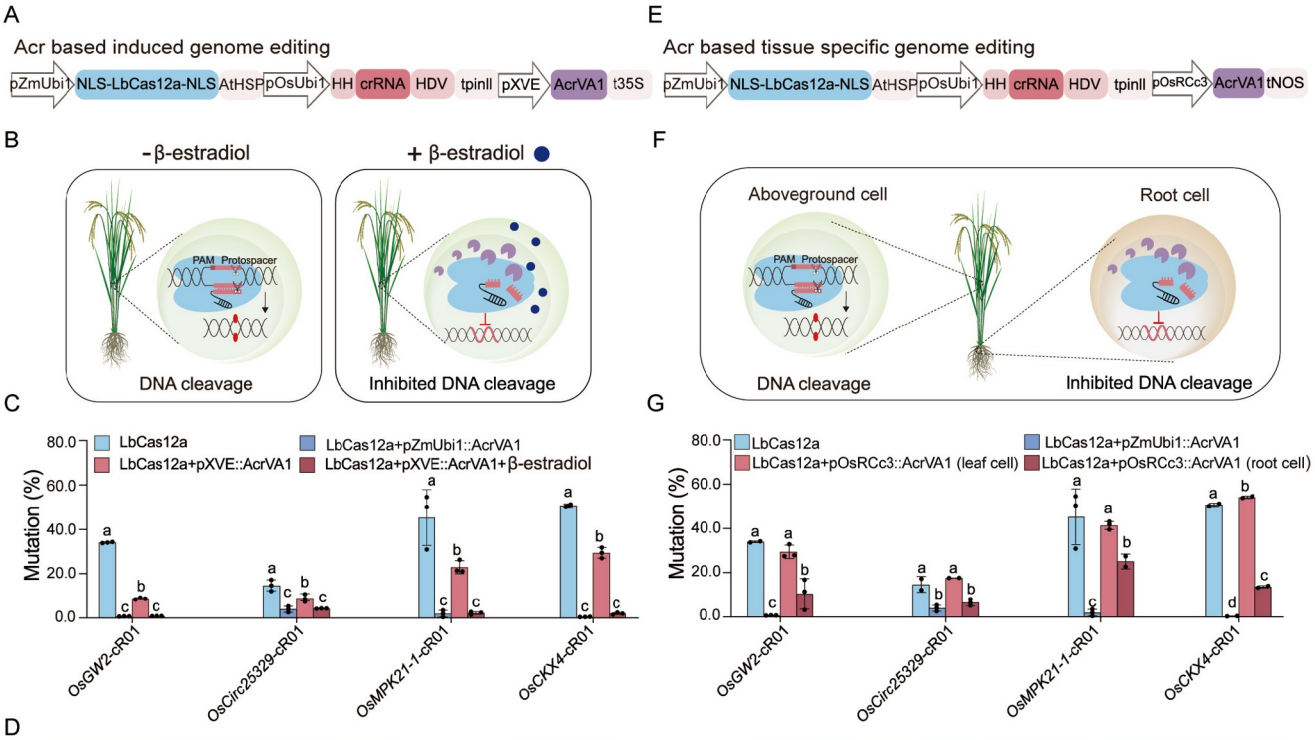

D

Targeted sites	LbCas12a			LbCas12a+pZmUbi1::AcrVA1			LbCas12a+pXVE::AcrVA1			LbCas12a+pXVE::AcrVA1+β-estradiol		
	Tested T0	Mutation*	Bi-mutation*	Tested T0	Mutation	Bi-mutation	Tested T0	Mutation	Bi-mutation	Tested T0	Mutation	Bi-mutation
OsGW2-cR01	22	14; 63.6%	7; 31.8%	19	3; 15.8%	1; 5.3%	18	3; 16.7%	1; 5.6%	20	2; 10.0%	0; 0.0%
OsCirc25329-cR01	22	13; 59.1%	7; 31.8%	19	1; 5.3%	0; 0.0%	18	9; 50.0%	2; 11.1%	20	4; 20.0%	2; 10.0%
OsMPK21-1-cR01	22	17; 77.3%	12; 54.6%	19	1; 5.3%	0; 0.0%	18	7; 38.9%	3; 16.7%	20	2; 10.0%	2; 10.0%
OsCKX4-cR01	22	19; 86.4%	16; 72.7%	19	1; 5.3%	0; 0.0%	18	10; 55.6%	8; 44.4%	20	7; 35.0%	2; 10.0%

*: (number; ratio)

Figure 5. Fine-tuning and tissue-specific genome editing in rice by using LbCas12a and AcrVA1. A, Schematic of the AcrVA1 based induced genome editing, dual RNA polymerase II promoter for LbCas12a and crRNA expression. The AcrVA1 is driven by an estrogen inducible promoter. B, Diagram showing the results of AcrVA1 based induced genome editing in plant cell without estradiol or with estradiol. C, Editing efficiency of protoplasts transformed with the LbCas12a nucleases without anti-CRISPR or with two different AcrVA1 expression editor in four sites. Editing efficiency was quantified by NGS of PCR amplicons. Each dot represents a biological replicate. Each target contains three biological replicates. Error bars represent the mean values±SD. Different small letters indicate significant differences (P<0.5; one-way ANOVA, Dunnett's test). D, The mutant rates of LbCas12a nucleases without anti-CRISPR or with two different AcrVA1 expression editor in four sites. E, Schematic of the AcrVA1 based tissue specific genome editing, dual RNA polymerase II promoter for LbCas12a and crRNA expression. The AcrVA1 is driven by a root specific promoter pOsRCc3. F, Diagram showing the results of AcrVA1 based root specific genome editing in aboveground cell and root cell. G, Editing efficiency of protoplasts transformed with the LbCas12a and two different AcrVA1 expression editor in four sites. Editing efficiency was quantified by NGS of PCR amplicons. Each dot represents a biological replicate. Each target contains two or three biological replicates. Error bars represent the mean values±SD. Different small letters indicate significant differences (P<0.5; one-way ANOVA, Dunnett's test).

by dLbCas12a-mediated CRISPRa (A2 cassette), a cassette expressing the dLbCas12a CRISPRa (B1 cassette), a cassette expressing AcrVA1 (C1 cassette), and a cassette conferring inducible expression of AcrVA1 by estrogen (C2 cassette; note the expression box for chimeric estrogen receptor protein activator (XVE) is located downstream of the terminator of the AcrVA1 expression cassette (not shown)) (Figure 6C). Based on these cassettes, we could create four major logic gates: TRUE (A1), FALSE (A2), YES (A2+B1), and IMPLY (A2+B1+C1); In addition, 'YES' and 'IMPLY' logic gates can be alternatively generated by using inducible expression of AcrVA1 (Figure 6C and D). We tested these logic gates plasmids in rice protoplasts. The eYFP signals appeared to faithfully represent the logic gate design (Figure 6E), and the eYFP readout was further quantified by normalizing to mCherry (Figure 6F). In our logic gate design, we also expressed crRNAs to target the promoters of *OsER1*, *OsGW7*, *OsWaxy*, and *OsMIR528* for transcriptional activation. However, we found that with the presence of the XVE promoter, with or without addition of β-estradiol, there was strong repression of CRISPRa (Figure 6G), suggesting that leaky expression of AcrVA1 exerted a much stronger on interference of CRISPRa.

DISCUSSION

With the rapid development of the CRISPR-Cas systems for diverse applications in animals (Asad et al., 2022; Fu et al., 2013; Kaminski et al., 2016; Miyamoto et al., 2024; Yang et al., 2017; Yin et al., 2017) and plants (Fan et al., 2024; Lee et al., 2019b; Li et al., 2020; Liang et al., 2023; Liu et al., 2022; Ren et al., 2023; Tang et al., 2024; Tang and Zhang, 2023; Xu et al., 2020; Zhong et al., 2023; Zhong et al., 2019; Zhou et al., 2019; Zhou et al., 2022), the necessity of controlling the CRISPR-Cas systems has been revealed. Anti-CRISPR or Acr proteins are

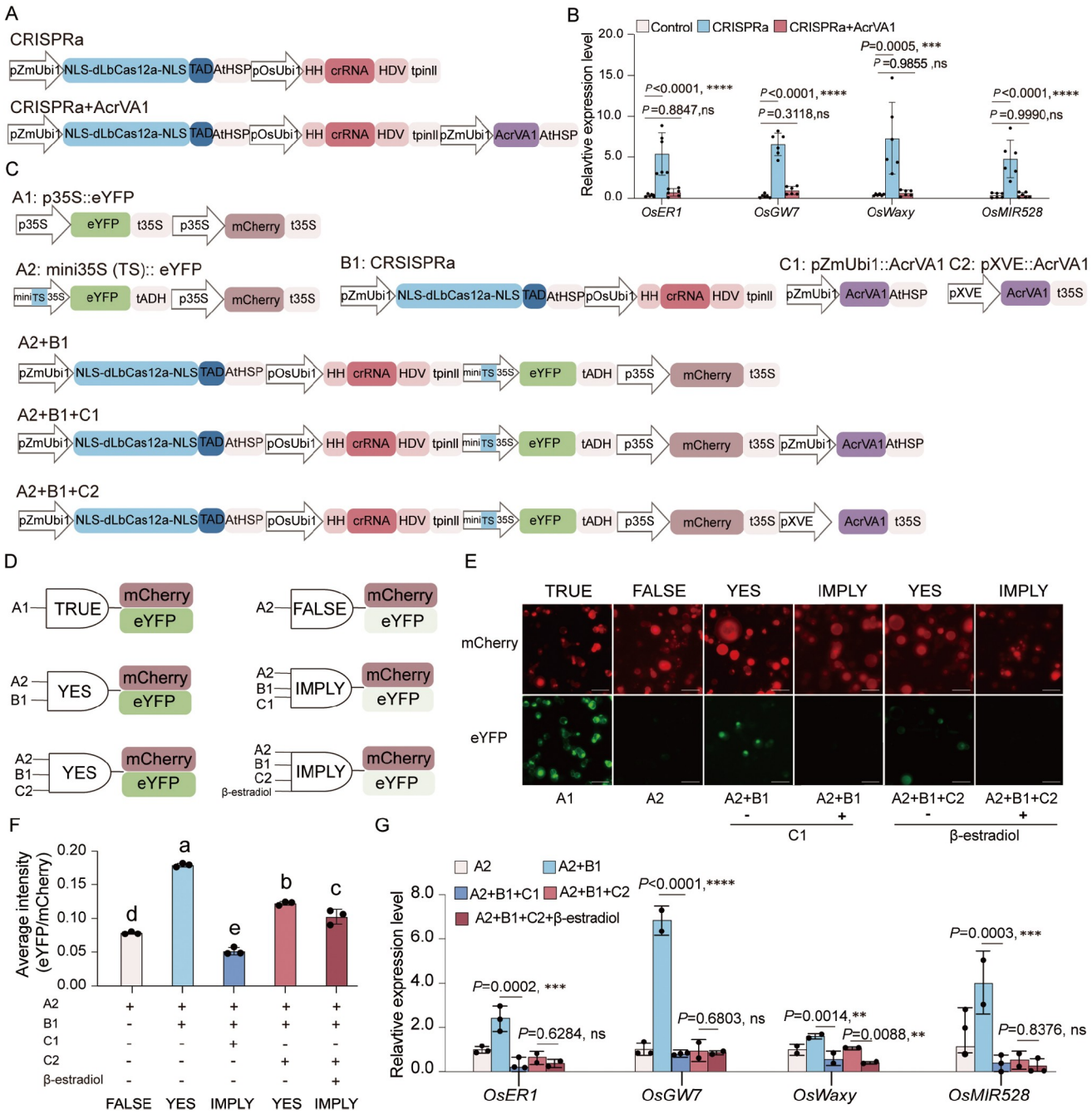

Figure 6. Efficient in planta suppression of CRISPRa by AcrVA1 and its use for construction of a synthetic circuit. A, Schematic of the CRISPRa and CRISPRa+AcrVA1, dual RNA polymerase II promoter for LbCas12a and crRNA expression. In CRISPRa+AcrVA1, the AcrVA1 is driven by RNA polymerase II promoter, TAD refers to the transcriptional activation domain. B, Transcriptional activation by CRISPRa and transcription activation is inhibited by CRISPRa+AcrVA1 in *OsER1*, *OsGW7*, *OsWaxy* and *OsMIR528* in rice. Each dot represents a replicate. each target contains three biological replicates, each biological contains two technology replicates. Error bars represent the mean values±SD (ns, $P>0.05$; ***, $P<0.001$; ****, $P<0.0001$, one-way ANOVA, Dunnett's test). C, Schematic diagram of constructs components in synthetic genetic circuits. A1: the mCherry and eYFP (eYFP, enhanced green fluorescence protein;) is driven by the cauliflower mosaic virus 35S promoter; A2: the mCherry is driven by the cauliflower mosaic virus 35S promoter; the eYFP is driven by a minimal plant promoter (positions –66 to +18 of the cauliflower mosaic virus (CaMV) 35S promoter), TS refers to the target sites of CRISPRa system based on dLbCas12a, and the sequence is PAM+crRNA; B1: CRISPRa; C1: AcrVA1 driven by RNA polymerase II promoter; C2: AcrVA1 driven by an estrogen inducible promoter. D, Schematic of synthetic genetic circuit. E, Representative images of mCherry and eYFP expressing protoplasts in different synthetic genetic circuit in rice protoplast. F, Normalized eYFP/mCherry ratios of different synthetic genetic circuit in rice protoplast. Each dot represents a biological replicate. Each target contains three biological replicates. Different small letters indicate significant differences ($P>0.05$. one-way ANOVA, Dunnett's test). G, Transcriptional activation by CRISPRa and transcription activation is inhibited by CRISPRa+AcrVA1 (expression by induced expression of promoters) in *OsER1*, *OsGW7*, *OsWaxy* and *OsMIR528* in rice. Each dot represents a replicate. each target contains two or three biological replicates. Error bars represent the mean values±SD (ns, $P>0.05$; *, $P<0.05$; **, $P<0.01$; ***, $P<0.001$; ****, $P<0.0001$, unpaired *t* test).

natural effectors evolved to inhibit CRISPR-Cas systems (Bondy-Denomy et al., 2013). At present, the main methods for discovering Acr genes include: 1) using aca/acr gene search (Bondy-Denomy et al., 2013; Pawluk et al., 2016b; Pinilla-Redondo et al., 2020), 2) searching in bacterial genomes with self-targeting spacers (Hynes et al., 2017; Marino et al., 2018;

https://doi.org/10.1007/s11427-024-2704-7

Watters et al., 2018; Watters et al., 2020), 3) searching in phage genomes resistant to CRISPR (Meeske et al., 2020), and 4) Applying high-throughput screening platforms (Jia and Patel, 2021). After obtaining candidate Acr proteins, multiple *in vitro* and *in vivo* experiments are needed to quickly screen and confirm these proteins (Forsberg et al., 2019; Pawluk et al., 2016a; Rauch et al., 2017; Song et al., 2023; Song et al., 2022; Watters et al., 2020). For example, AcrIIA13-15, AcrVA1, AcrVA4, and AcrVA5 were screened and identified via the TXTL screening reactions(Watters et al., 2018; Watters et al., 2020); AcrIE5-7, AcrIF11,12, AcrIIA12, AcrIIA16-19, AcrVA1, AcrVA2, and AcrVA3 were validated by phage plaque assay (Bondy-Denomy et al., 2013; Mahendra et al., 2020; Marino et al., 2018; Osuna et al., 2020); AcrIIC1-5, AcrIIA1-4, AcrIIA7-11, and AcrIIA22-34 were identified by using plasmid interference systems (Forsberg et al., 2019; Forsberg et al., 2021; Pawluk et al., 2016a; Rauch et al., 2017; Song et al., 2023; Song et al., 2022; Uribe et al., 2019).

In this study, we established an efficient plasmid interference system for rapid screening of type V-A Acr proteins, and this approach was not used in identifying type V-A Acr proteins before. We tested three known type V-A Acr proteins (AcrVA1, AcrVA4, and AcrVA5) and 6 promising Acr candidate proteins (AcrC01 to AcrC06) identified from our computational pipeline. These Acr proteins were further assessed in rice, both transiently and stably, for their potential inhibitory effects on CRISPR-Cas12a mediated genome editing. Among them, AcrVA1 exhibited strong inhibitory activity against LbCas12a and Mb2Cas12a in *E. coli* and rice, and our results are consistent with those observed in prokaryotes and human cells (Marino et al., 2018; Watters et al., 2018). The identification of AcrVA1 as a potent anti-CRISPR protein for both LbCas12a and Mb2Cas12a is very important because LbCas12a is the most robust and widely used Cas12a in plant genome engineering (Liang et al., 2023; Ren et al., 2023; Tang et al., 2018; Tang et al., 2017; Tang et al., 2019; Zheng et al., 2023; Zhong et al., 2018; Zhou et al., 2023) and Mb2Cas12a and its variant greatly expand the targeting range in plant genome engineering (Hui et al., 2024; Zhang et al., 2021). Based on the plasmid interference system, we detected anti-CRISPR activity of AcrVA5 on Mb2Cas12a, but not on LbCas12a (Figure 1E–H). Interestingly, AcrVA5 exerted inhibitory effects on genome editing activity of both LbCas12a and Mb2Cas12a in stable transgenic rice plants (Figure 2F and H), while such effects were not detected in rice protoplasts (Figure 2E and G). These data suggest the stable transformation system is more sensitive for the detection of anti-CRISPR effects, especially for Acr proteins with weak activities. Indeed, in stable transgenic plants, we were able to see mild inhibitory activity of AcrVA4 on LbCas12a, but not on Mb2Cas12a (Figure 2F and H).

Our observation of various levels of inhibitory effects by these three Acr proteins can be first explained by their different modes of action. AcrVA1 can directly destroy crRNAs, while AcrVA4 and AcrVA5 only introduce small modifications the CRISPR-Cas12a RNP complex (Figure 1C). Furthermore, AcrVA1 originates from a single locus, while AcrVA4 and AcrVA5 originate from the same locus and may have a complementary and additive effect by working together (Marino, 2023; Marino et al., 2018; Watters et al., 2018). Our result is consistent with the previous observation that AcrVA1 can perform multiple rounds of cleavage and truncate up to 95% of Cas12a-bound crRNAs, even at sub-stoichiometric levels (Knott et al., 2019b). By contrast, AcrVA4 and AcrVA5 have a greater dependence on concentration: both Acr proteins exhibit better activity at high concentrations (Dong et al., 2019; Watters et al., 2018; Zuo et al., 2000). In addition, AcrVA5 was found only in *Moraxella bovoculi* strains (strains 22581, 28389, and 33362) that appear to have lost their deacetylases (Dong et al., 2019; Watters et al., 2018; Zuo et al., 2000), it is possible that prokaryotic deacetylase present in *E. coli* (Starai and Escalante-Semerena, 2004; Xu et al., 2019) or a similar enzyme encoded by *OsHDA714* in rice (Xu et al., 2021) may reverse the acetylation of Cas12a by AcrVA5, hence significantly masking its inhibitory effect in both systems. Out of six new Acr proteins tested, only AcrC03, with a predicted compact structure (Figure S1C in Supporting Information), displayed some inhibitory activity on LbCas12a meditated genome editing (Figure 2D). Further investigation of AcrC03's potential anti-CRISPR activity and mode of action is needed.

Since AcrVA1 was confirmed to have excellent anti-CRISPR-Cas12a activity in plants, we focused on the use of AcrVA1 to control CRISPR-Cas12a genome editing and CRISPRa. We first demonstrated that AcrVA1, when co-expressed, could be used for mitigating off-target effects of CRISPR-Cas12a, based on the WGS analysis of edited rice plants (Figure 3). That promoted us to further show, in a sequential transformation approach, that AcrVA1-expressing plants were resistant to LbCas12a mediated genome editing (Figure 4). Furthermore, we demonstrated inducible anti-CRISPR effect in both rice cells and plants (Figure 5A–D). Altogether, these experiments showcased the use of efficient anti-CRISPR proteins for sophisticated control of CRISPR-Cas12a mediated genome editing applications. CRISPR-Cas12a can be used to make efficient gene drive systems to manipulate insect population (Sanz Juste et al., 2023). Under complex feeding and behavioral conditions, anti-driven inhibition based on AcrIIA4 inhibits gene driven transmission in the age-structured population of *Anopheles gambiae* (D'Amato et al., 2024). Should a gene drive be implemented in plants, we anticipate the possible use of AcrVA1 to block the spread of a Cas12a-based gene drive system into unintended populations. Many potential applications of Acr proteins rely on their ability to regulate genetic circuits based on CRISPRa and CRISPRi (Kawasaki et al., 2023; Kempton et al., 2020; Nakamura et al., 2019; Yu and Marchisio, 2021). In this study, we also showed AcrVA1 can strongly inhibit Cas12a-based CRISPRa, as shown in tobacco cells (Calvache et al., 2022). Based on this principle, we demonstrated the engineering of logic gates and control of endogenous gene expression in plant cells (Figure 6). Previously, inducible and tissue-specific genome editing was demonstrated with CRISPR-Cas9 in plants (Decaestecker et al., 2019; Wang et al., 2020). Here, we demonstrated inducible and tissue-specific inhibition of Cas12a genome editing and CRISPRa, providing an opposite means of regulation.

Because AcrVA1 targets crRNAs which are very conserved among different CRISPR-Cas12a systems, we anticipate AcrVA1 to be one of the most powerful and broad-spectrum Cas12a inhibitor, which will not only inhibit engineered high-activity LbCas12a variants such as ttLbCas12a (Huang et al., 2021; Schindele et al., 2023) and LbCas12a-RRV (Zhang et al., 2023), but also other Cas12a orthologs beyond LbCas12a and Mb2Cas12a (Li et al., 2023; Zhang et al., 2021). The systems that we developed and demonstrated suggest promising applications of AcrVA1 in plant genome engineering and synthetic biology. However, not all applications require the use of a strong Acr

protein like AcrVA1. For example, AcrVA5 can significantly reduce off-target effects (Figure 3D–H), while not severely affect the on-target editing efficiency (Figure 2D–H). It may be more practical to use a weaker Acr protein such as AcrVA5, rather than a stronger one such as AcrVA1, for mitigating off-target effects in plants. Hence, it is worthwhile to screen for additional novel Acr proteins with various inhibitory activities on different Cas12a proteins in plants, based on the pipeline that we established in *E. coli* and in plants (Figures 1 and 2).

METHODS

Data mining

To identify novel anti-CRISPR (Acr) genes, we developed a decision-tree-based model that incorporate five features, including gene length, gene location (being contained in genome islands or prophages), codon usage bias, gene function, and the presence of adjacent HTH (Helix-turn-helix) containing proteins near our target protein-coding genes. Genome islands were annotated using IslandViewer4 (Bertelli et al., 2017), and prophages were detected using PHASTER (Arndt et al., 2016). hmmscan were used to identify whether the downstream protein-coding genes encode the HTH domain. Furthermore, Proksee (Grant et al., 2023) analysis of the genome revealed that the candidate genes are in the vicinity of genomic hotspots, such as transfer and recombination of mobileOG categories. Moreover, we further investigated the gene distribution by performing BLAST analysis on the candidate proteins against the NR database, revealing their phylum-specific distribution. The protein structures encoded by these genes, as predicted by RoseTTAFold, display a significant enrichment in helix and loop structures.

Construction of the vectors

The vectors used in bacteria were constructed by Gibson assembly. DNA sequences were synthesized and cloned into bacterial expression vectors. The vectors used in plant were constructed based on the backbone of pTrans_210d (Addgene Plasmid #91109). To construct the singular editing vectors, LbCas12a gene was rice codon optimized and synthesized in DNA fragments, which were cloned into pTX770 by Golden Gate Assembly to generate pYSS125. To obtain the singular target site expression cassette named pHY14, the synthesized oligos were annealed and assembled into pTX771 by Golden Gate Assembly. To obtain the Acr proteins expression cassette named MOD_C, the DNA sequences of the nine Acr genes were rice codon optimized and synthesized. Then the DNA fragments were cloned into pMOD_C4810ec, separately, by Golden Gate Assembly to generate pHY37-43, pHY73, and pHY74. We assembled the expression vectors pHY44-50, pHY75, pHY77 and pHY31 (control, No Acr) by Golden Gate Assembly using pTrans_210d, pYSS125 (LbCas12a expression cassette), pHY14 (crRNA expression cassette), and MOD_C (Acr proteins expression cassette or control).

Multiplex LbCas12a and Mb2Cas12a editing vectors pHY263-266 and pHY289-293 were constructed by Golden Gate Assembly of pTrans_210d, MOD_A (pYSS125: LbCas12a expression cassette or pYSS119: Mb2Cas12a expression cassette), MOD_B (pHY239: multiplex crRNA expression cassette or pHY241: multiplex crRNA expression cassette), and MOD_C (Acr proteins expression cassette or control).To construct the MOD_B with crRNA sequences for multiplex editing, three fragments (crRNA01-HDV-HH-DR-crRNA02 (4 bp), crRNA02-HDV-HH-DR-crRNA03 (4 bp), crRNA03-HDV-HH-DR-crRNA04) were synthesized by Sangon Biotech (Shanghai, China), flanked with *BsaI* restriction enzyme sites. The final T-DNA recombinant expression vectors were constructed with Golden Gate reactions. Using the identical vector construction method, we created the fine-tuning and tissue-specific genome editing vectors, CRISPRa vectors and genetic circuits vectors. Sanger sequencing was used to confirm the integrity of all vectors. Table S4 in Supporting Information provides a comprehensive list of constructs used in this study. Table S5 in Supporting Information provides a comprehensive list of the crRNAs utilized in this study. Table S6 in Supporting Information provides a comprehensive list of the Oligos and sequence utilized in this study.

Plasmid interference assay

The Acr protein expression vectors and empty control vector (no Acr) were first transformed in *E. coli* DH5α to make the competent cell with ampicillin selection. Then, the plasmid containing Cas12a with crRNA and the plasmid containing target site spacer without (W/o) PAM or spacer with (W/) PAM were transformed into the competent cell at the same time by heat shock transformation. The co-transformed *E. coli* were selected on solid LB medium containing kanamycin, ampicillin, and spectinomycin. The resulting colonies were counted using ImageJ (https://imagej.net/) Software.

Rice protoplast transformation

The Japonica cultivar Nipponbare rice seedlings were cultivated on 1/2 MS solid medium for a period of 10-12 days in the absence of light at a temperature of 28°C. The preparation and transformation of rice protoplasts were conducted in accordance with our previously published protocols (Ren et al., 2021a; Tang et al., 2017). In brief, leaves or roots of rice seedlings were finely sliced into strips measuring 0.5–1.0 mm and immersed in an enzyme solution. After a 30 min vacuum infiltration, the sliced tissue underwent incubation in darkness at 25°C with gentle agitation (60–80 rpm) for 6 h. The resulting digestion mixture was then filtered through a 40 μm nylon mesh. Following two washes with W5 washing buffer, the protoplasts were meticulously examined and counted under a microscope. The final concentration of protoplasts was adjusted to 2×10^6 per milliliter. For protoplast transformation, 30 μg of plasmid DNA in 30 μL (1 μg μL^{-1}, prepared using the Qiagen Midiprep kit) was gently combined with 200 μL of protoplasts and 230 μL of 40% PEG transformation buffer. After a 30 min incubation in darkness, the reactions were terminated by the addition of 900 μL W5 washing buffer. The protoplasts were then subjected to low-speed centrifugation and transferred to a 12-well culture plate for further incubation in darkness at 32°C for a duration of 48 h.

Rice stable transformation

The Japonica cultivar Nipponbare was used for the stable *Agrobacterium*-mediated transformation of rice, based on a protocol established in our lab (Lowder et al., 2015; Zhou et

al., 2021). Briefly, rice seeds underwent dehulling, sterilization, and subsequent cultivation on solid N6-D medium. Pre-cultured rice calli were subjected to transformation by inoculating *Agrobacterium EHA105* carrying the recombinant expression vector. Following a 3-day co-cultivation of rice calli with *Agrobacterium* in the co-culture medium, the calli were rinsed with sterile water and transferred to N6-S medium for a selective period of 2 weeks. The newly propagated calli were then transferred to RE-III medium and cultured for an additional 2 weeks. Resistant calli were transferred to fresh RE-III medium every two weeks until regenerated plants were successfully achieved.

Detection and quantification of genome editing

The harvested rice protoplasts or tissue from stable transgenic plants were used for DNA extraction utilizing the CTAB method (Stewart and Via, 1993). Quantification of targeted mutagenesis was carried out through next-generation sequencing (NGS) of PCR amplicons utilizing barcoded primers (Ren et al., 2021b; Wu et al., 2022a). Sequencing of the PCR amplicons was performed on an Illumina HiseqX platform. Subsequent data analysis was executed using the CRISPRMatch (You et al., 2018) and CrisprStitch (Han et al., 2024). To genotype T_0 lines, Sanger sequencing of PCR amplicons was applied, adhering to a previously established protocol (Zhou et al., 2017). The obtained sequencing data were then analyzed using the CRISPR-GE DSDecodeM software (Xie et al., 2017).

RNA extraction and qRT-PCR

RNA extraction was executed utilizing the SteadyPure Plant RNA Isolation Kit (Accurate Biology, China), followed by reverse transcription using the HiScript III 1st Strand cDNA Synthesis Kit (Vazyme, China). Real-time quantitative polymerase chain reaction (qPCR) was carried out by employing the ChamQ Universal SYBR qPCR Master Mix (Vazyme, China) by following the manufacturer's guidelines, with *OsActin* mRNA used as an internal control. The $2^{-\Delta\Delta Ct}$ method was used to calculate the relative levels of gene expression. To ensure reproducibility, two biological replicates (comprising two independent mutant leaves) were examined. The experiment was independently conducted three times, yielding similar and consistent results.

Whole-genome sequencing and data analysis

The rice plants identified through screening with Sanger sequencing were transplanted into growth chambers and cultivated at 28°C with a 12-hour light/12-hour dark cycle. After 5–6 weeks of cultivation, 10–15 cm leaf samples were collected from each plant, placed in self-sealing bags or 50 mL centrifuge tubes, rapidly frozen in liquid nitrogen, and stored in a –80°C ultra-low temperature freezer. Two to six leaf samples were collected from each plant for backup. The DNA samples were sent to Novogene Company in Beijing, using the Illumina NovaSeq platform for resequencing. The average sequencing data for each sample was 20 Gb, with an average depth of approximately 50× to 60×. We followed a similar WGS analysis pipeline as we previously demonstrated (Wu et al., 2022a; Wu et al., 2022b) . Briefly, the returned whole-genome sequencing data underwent quality control and filtering using SKEWER software. The filtered data were aligned to the rice reference sequence using BWA software. Picard and Samtools were employed to mark duplicate reads and generate BAM files. The GATK software was used for quality correction of insertions, deletions, and base substitutions. The analysis of whole-genome single nucleotide variations (SNVs) was conducted using LoFreq, MuTect2, and VarScan2 software. The analysis of whole-genome insertions and deletions (InDels) was performed using MuTect2, VarScan2, and Pindel software. Bedtools and BCFtools were used to obtain files for SNVs and indels. CRISPR RGEN Tools were utilized to predict potential off-target sites in the rice genome. Data processing, analysis, and graphical representation were carried out using the R and Python.

Data analysis

The data were analyzed with the GraphPad Prism 9.0 software, and the figures were made using the Adobe Photoshop and Adobe Illustrator software.

Data availablitily statement

Backbone vector pTrans_210d (Addgene Plasmid #91109) is available from Addgene. The high-throughput sequencing and WGS data sets generated from this study are available at Beijing Institute of Genomics Data Center (http://bigd.big.ac.cn) under BioProject PRJCA023882. The code of Acr proteins mining has been uploaded to the Github site https://github.com/pudongkai/acrDetector.

Compliance and ethics

The authors declare no competing interests.

Acknowledgement

This work was supported by the Biological Breeding-Major Projects (2023ZD04074), National Natural Science Foundation of China (32270433, 32101205 and 32072045), Natural Science Foundation of Sichuan Province (2022NSFSC0143). It is also supported by the NSF Plant Genome Research Program (IOS-2029889 and IOS-2132693).

Supporting information

The supporting information is available online at https://doi.org/10.1007/s11427-024-2704-7. The supporting materials are published as submitted, without typesetting or editing. The responsibility for scientific accuracy and content remains entirely with the authors.

References

Arndt, D., Grant, J.R., Marcu, A., Sajed, T., Pon, A., Liang, Y., and Wishart, D.S. (2016). PHASTER: a better, faster version of the PHAST phage search tool. Nucleic Acids Res 44, W16–W21.

Asad, M., Liu, D., Li, J., Chen, J., and Yang, G. (2022). Development of CRISPR/Cas9-mediated gene-drive construct targeting the phenotypic gene in *Plutella xylostella*. Front Physiol 13, 938621.

Bae, S., Park, J., and Kim, J.S. (2014). Cas-OFFinder: a fast and versatile algorithm that searches for potential off-target sites of Cas9 RNA-guided endonucleases. Bioinformatics 30, 1473–1475.

Basgall, E.M., Goetting, S.C., Goeckel, M.E., Giersch, R.M., Roggenkamp, E., Schrock, M.N., Halloran, M., and Finnigan, G.C. (2018). Gene drive inhibition by the anti-CRISPR proteins AcrIIA2 and AcrIIA4 in *Saccharomyces cerevisiae*. Microbiology 164, 464–474.

Bertelli, C., Laird, M.R., Williams, K.P., Lau, B.Y., Hoad, G., Winsor, G.L., and Brinkman, F.S. (2017). IslandViewer 4: expanded prediction of genomic islands for larger-scale datasets. Nucleic Acids Res 45, W30–W35.

Bondy-Denomy, J., Pawluk, A., Maxwell, K.L., and Davidson, A.R. (2013). Bacteriophage genes that inactivate the CRISPR/Cas bacterial immune system. Nature 493, 429–432.

Bubeck, F., Hoffmann, M.D., Harteveld, Z., Aschenbrenner, S., Bietz, A., Waldhauer, M.C., Börner, K., Fakhiri, J., Schmelas, C., Dietz, L., et al. (2018). Engineered anti-CRISPR proteins for optogenetic control of CRISPR–Cas9. Nat Methods 15, 924–927.

Calvache, C., Vazquez-Vilar, M., Selma, S., Uranga, M., Fernández-del-Carmen, A., Daròs, J.A., and Orzáez, D. (2022). Strong and tunable anti-CRISPR/Cas activities in plants. Plant Biotechnol J 20, 399–408.
Campa, C.C., Weisbach, N.R., Santinha, A.J., Incarnato, D., and Platt, R.J. (2019). Multiplexed genome engineering by Cas12a and CRISPR arrays encoded on single transcripts. Nat Methods 16, 887–893.
D'Amato, R., Taxiarchi, C., Galardini, M., Trusso, A., Minuz, R.L., Grilli, S., Somerville, A.G.T., Shittu, D., Khalil, A.S., Galizi, R., et al. (2024). Anti-CRISPR Anopheles mosquitoes inhibit gene drive spread under challenging behavioural conditions in large cages. Nat Commun 15, 952.
Decaestecker, W., Buono, R.A., Pfeiffer, M.L., Vangheluwe, N., Jourquin, J., Karimi, M., Van Isterdael, G., Beeckman, T., Nowack, M.K., and Jacobs, T.B. (2019). CRISPR-TSKO: a technique for efficient mutagenesis in specific cell types, tissues, or organs in *Arabidopsis*. Plant Cell 31, 2868–2887.
Dong, D., Guo, M., Wang, S., Zhu, Y., Wang, S., Xiong, Z., Yang, J., Xu, Z., and Huang, Z. (2017). Structural basis of CRISPR–SpyCas9 inhibition by an anti-CRISPR protein. Nature 546, 436–439.
Dong, L., Guan, X., Li, N., Zhang, F., Zhu, Y., Ren, K., Yu, L., Zhou, F., Han, Z., Gao, N., et al. (2019). An anti-CRISPR protein disables type V Cas12a by acetylation. Nat Struct Mol Biol 26, 308–314.
Fan, T., Cheng, Y., Wu, Y., Liu, S., Tang, X., He, Y., Liao, S., Zheng, X., Zhang, T., Qi, Y., et al. (2024). High performance TadA-8e derived cytosine and dual base editors with undetectable off-target effects in plants. Nat Commun 15, 5103.
Forsberg, K.J., Bhatt, I.V., Schmidtke, D.T., Javanmardi, K., Dillard, K.E., Stoddard, B. L., Finkelstein, I.J., Kaiser, B.K., and Malik, H.S. (2019). Functional metagenomics-guided discovery of potent Cas9 inhibitors in the human microbiome. eLife 8, e46540.
Forsberg, K.J., Schmidtke, D.T., Werther, R., Uribe, R.V., Hausman, D., Sommer, M.O. A., Stoddard, B.L., Kaiser, B.K., Malik, H.S., and Meeske, A.J. (2021). The novel anti-CRISPR AcrIIA22 relieves DNA torsion in target plasmids and impairs SpyCas9 activity. PLoS Biol 19, e3001428.
Fu, Y., Foden, J.A., Khayter, C., Maeder, M.L., Reyon, D., Joung, J.K., and Sander, J.D. (2013). High-frequency off-target mutagenesis induced by CRISPR-Cas nucleases in human cells. Nat Biotechnol 31, 822–826.
Garcia, B., Lee, J., Edraki, A., Hidalgo-Reyes, Y., Erwood, S., Mir, A., Trost, C.N., Seroussi, U., Stanley, S.Y., Cohn, R.D., et al. (2019). Anti-CRISPR AcrIIA5 potently inhibits all Cas9 homologs used for genome editing. Cell Rep 29, 1739–1746.e5.
Grant, J.R., Enns, E., Marinier, E., Mandal, A., Herman, E.K., Chen, C., Graham, M., Van Domselaar, G., and Stothard, P. (2023). Proksee: in-depth characterization and visualization of bacterial genomes. Nucleic Acids Res 51, W484–W492.
Griffith, A.L., Zheng, F., McGee, A.V., Miller, N.W., Szegletes, Z.M., Reint, G., Gademann, F., Nwolah, I., Hegde, M., Liu, Y.V., et al. (2023). Optimization of Cas12a for multiplexed genome-scale transcriptional activation. Cell Genomics 3, 100387.
Grissa, I., Vergnaud, G., and Pourcel, C. (2007). The CRISPRdb database and tools to display CRISPRs and to generate dictionaries of spacers and repeats. BMC BioInf 8, 172.
Han, Y., Liu, G., Wu, Y., Bao, Y., Zhang, Y., and Zhang, T. (2024). CrisprStitch: fast evaluation of the efficiency of CRISPR editing systems. Plant Commun 5, 100783.
Harrington, L.B., Doxzen, K.W., Ma, E., Liu, J.J., Knott, G.J., Edraki, A., Garcia, B., Amrani, N., Chen, J.S., Cofsky, J.C., et al. (2017). A broad-spectrum inhibitor of CRISPR-Cas9. Cell 170, 1224–1233.e15.
He, Y., Han, Y., Ma, Y., Liu, S., Fan, T., Liang, Y., Tang, X., Zheng, X., Wu, Y., Zhang, T., et al. (2024). Expanding plant genome editing scope and profiles with CRISPR-FrCas9 systems targeting palindromic TA sites. Plant Biotechnol J pbi.14363.
Hirosawa, M., Fujita, Y., and Saito, H. (2019). Cell-type-specific CRISPR activation with microRNA-responsive AcrllA4 switch. ACS Synth Biol 8, 1575–1582.
Hoffmann, M.D., Aschenbrenner, S., Grosse, S., Rapti, K., Domenger, C., Fakhiri, J., Mastel, M., Börner, K., Eils, R., Grimm, D., et al. (2019). Cell-specific CRISPR–Cas9 activation by microRNA-dependent expression of anti-CRISPR proteins. Nucleic Acids Res 47, e75.
Huang, T.K., Armstrong, B., Schindele, P., and Puchta, H. (2021). Efficient gene targeting in *Nicotiana tabacum* using CRISPR/SaCas9 and temperature tolerant LbCas12a. Plant Biotechnol J 19, 1314–1324.
Hui, F., Tang, X., Li, B., Alariqi, M., Xu, Z., Meng, Q., Hu, Y., Wang, G., Zhang, Y., Zhang, X., et al. (2024). Robust CRISPR/Mb2Cas12a genome editing tools in cotton plants. iMeta 3, e209.
Hwang, S., and Maxwell, K.L. (2023). Diverse mechanisms of CRISPR-Cas9 inhibition by type II anti-CRISPR proteins. J Mol Biol 435, 168041.
Hynes, A.P., Rousseau, G.M., Lemay, M.L., Horvath, P., Romero, D.A., Fremaux, C., and Moineau, S. (2017). An anti-CRISPR from a virulent streptococcal phage inhibits *Streptococcus pyogenes* Cas9. Nat Microbiol 2, 1374–1380.
Jeong, J.S., Kim, Y.S., Redillas, M.C.F.R., Jang, G., Jung, H., Bang, S.W., Choi, Y.D., Ha, S.H., Reuzeau, C., and Kim, J.K. (2013). *OsNAC5* overexpression enlarges root diameter in rice plants leading to enhanced drought tolerance and increased grain yield in the field. Plant Biotechnol J 11, 101–114.
Jia, N., and Patel, D.J. (2021). Structure-based functional mechanisms and biotechnology applications of anti-CRISPR proteins. Nat Rev Mol Cell Biol 22, 563–579.
Jinek, M., Chylinski, K., Fonfara, I., Hauer, M., Doudna, J.A., and Charpentier, E. (2012). A programmable dual-RNA–guided DNA endonuclease in adaptive bacterial immunity. Science 337, 816–821.
Kaminski, R., Bella, R., Yin, C., Otte, J., Ferrante, P., Gendelman, H.E., Li, H., Booze, R., Gordon, J., Hu, W., et al. (2016). Erratum: excision of HIV-1 DNA by gene editing: a proof-of-concept *in vivo* study. Gene Ther 23, 696.
Kawasaki, S., Ono, H., Hirosawa, M., Kuwabara, T., Sumi, S., Lee, S., Woltjen, K., and Saito, H. (2023). Programmable mammalian translational modulators by CRISPR-associated proteins. Nat Commun 14, 2243.
Kempton, H.R., Goudy, L.E., Love, K.S., and Qi, L.S. (2020). Multiple input sensing and signal integration using a split Cas12a system. Mol Cell 78, 184–191.e3.
Knott, G.J., Cress, B.F., Liu, J.J., Thornton, B.W., Lew, R.J., Al-Shayeb, B., Rosenberg, D.J., Hammel, M., Adler, B.A., Lobba, M.J., et al. (2019). Structural basis for AcrVA4 inhibition of specific CRISPR-Cas12a. eLife 8, e49110.
Knott, G.J., Thornton, B.W., Lobba, M.J., Liu, J.J., Al-Shayeb, B., Watters, K.E., and Doudna, J.A. (2019b). Broad-spectrum enzymatic inhibition of CRISPR-Cas12a. Nat Struct Mol Biol 26, 315–321.
Kunin, V., Sorek, R., and Hugenholtz, P. (2007). Evolutionary conservation of sequence and secondary structures in CRISPR repeats. Genome Biol 8, R61.
Lee, J., Mir, A., Edraki, A., Garcia, B., Amrani, N., Lou, H.E., Gainetdinov, I., Pawluk, A., Ibraheim, R., Gao, X.D., et al. (2018). Potent Cas9 Inhibition in bacterial and human cells by AcrIIC4 and AcrIIC5 anti-CRISPR proteins. mBio 9, e02321-18.
Lee, J., Mou, H., Ibraheim, R., Liang, S.Q., Liu, P., Xue, W., and Sontheimer, E.J. (2019a). Tissue-restricted genome editing *in vivo* specified by microRNA-repressible anti-CRISPR proteins. RNA 25, 1421–1431.
Lee, K., Zhang, Y., Kleinstiver, B.P., Guo, J.A., Aryee, M.J., Miller, J., Malzahn, A., Zarecor, S., Lawrence-Dill, C.J., Joung, J.K., et al. (2019b). Activities and specificities of CRISPR/Cas9 and Cas12a nucleases for targeted mutagenesis in maize. Plant Biotechnol J 17, 362–372.
Li, G., Zhang, Y., Dailey, M., and Qi, Y. (2023). Hs1Cas12a and Ev1Cas12a confer efficient genome editing in plants. Front Genome Ed 5, 1251903.
Li, S., Zhang, Y., Xia, L., and Qi, Y. (2020). CRISPR-Cas12a enables efficient biallelic gene targeting in rice. Plant Biotechnol J 18, 1351–1353.
Liang, D., Liu, Y., Li, C., Wen, Q., Xu, J., Geng, L., Liu, C., Jin, H., Gao, Y., Zhong, H., et al. (2023). CRISPR/LbCas12a-mediated genome editing in soybean. Methods Mol Biol 2653, 39–52.
Liang, M., Sui, T., Liu, Z., Chen, M., Liu, H., Shan, H., Lai, L., and Li, Z. (2020). AcrIIA5 suppresses base editors and reduces their off-target effects. Cells 9, 1786.
Liu, H., Zhu, Y., Lu, Z., and Huang, Z. (2021). Structural basis of *Staphylococcus aureus* Cas9 inhibition by AcrIIA14. Nucleic Acids Res 49, 6587–6595.
Liu, L., Yin, M., Wang, M., and Wang, Y. (2019). Phage AcrIIA2 DNA mimicry: structural basis of the CRISPR and anti-CRISPR arms race. Mol Cell 73, 611–620.e3.
Liu, S., Sretenovic, S., Fan, T., Cheng, Y., Li, G., Qi, A., Tang, X., Xu, Y., Guo, W., Zhong, Z., et al. (2022). Hypercompact CRISPR–Cas12j2 (CasΦ) enables genome editing, gene activation, and epigenome editing in plants. Plant Commun 3, 100453.
Liu, Y., Yuan, G., Hyden, B., Tuskan, G.A., Abraham, P.E., and Yang, X. (2023). Expanding the application of anti-CRISPR proteins in plants for tunable genome editing. Plant Physiol 192, 60–64.
Lowder, L.G., Zhang, D., Baltes, N.J., Paul Iii, J.W., Tang, X., Zheng, X., Voytas, D.F., Hsieh, T.F., Zhang, Y., and Qi, Y. (2015). A CRISPR/Cas9 toolbox for multiplexed plant genome editing and transcriptional regulation. Plant Physiol 169, 971–985.
Mahendra, C., Christie, K.A., Osuna, B.A., Pinilla-Redondo, R., Kleinstiver, B.P., and Bondy-Denomy, J. (2020). Broad-spectrum anti-CRISPR proteins facilitate horizontal gene transfer. Nat Microbiol 5, 620–629.
Makarova, K.S., Koonin, E.V. (2015). Annotation and classification of CRISPR-Cas systems. Methods Mol Biol 1311, 47–75.
Makarova, K.S., Wolf, Y.I., Iranzo, J., Shmakov, S.A., Alkhnbashi, O.S., Brouns, S.J.J., Charpentier, E., Cheng, D., Haft, D.H., Horvath, P., et al. (2020). Evolutionary classification of CRISPR–Cas systems: a burst of class 2 and derived variants. Nat Rev Microbiol 18, 67–83.
Marino, N.D. (2023). Phage against the machine: discovery and mechanism of type V anti-CRISPRs. J Mol Biol 435, 168054.
Marino, N.D., Zhang, J.Y., Borges, A.L., Sousa, A.A., Leon, L.M., Rauch, B.J., Walton, R.T., Berry, J.D., Joung, J.K., Kleinstiver, B.P., et al. (2018). Discovery of widespread type I and type V CRISPR-Cas inhibitors. Science 362, 240–242.
Mathony, J., Harteveld, Z., Schmelas, C., Upmeier zu Belzen, J., Aschenbrenner, S., Sun, W., Hoffmann, M.D., Stengl, C., Scheck, A., Georgeon, S., et al. (2020). Computational design of anti-CRISPR proteins with improved inhibition potency.

Nat Chem Biol 16, 725–730.
Meeske, A.J., Jia, N., Cassel, A.K., Kozlova, A., Liao, J., Wiedmann, M., Patel, D.J., and Marraffini, L.A. (2020). A phage-encoded anti-CRISPR enables complete evasion of type VI-A CRISPR-Cas immunity. Science 369, 54–59.
Miyamoto, H., Kobayashi, H., Kishima, N., Yamazaki, K., Hamamichi, S., Uno, N., Abe, S., Hiramuki, Y., Kazuki, K., Tomizuka, K., et al. (2024). Rapid human genomic DNA cloning into mouse artificial chromosome via direct chromosome transfer from human iPSC and CRISPR/Cas9-mediated translocation. Nucleic Acids Res 52, 1498–1511.
Nakamura, M., Srinivasan, P., Chavez, M., Carter, M.A., Dominguez, A.A., La Russa, M., Lau, M.B., Abbott, T.R., Xu, X., Zhao, D., et al. (2019). Anti-CRISPR-mediated control of gene editing and synthetic circuits in eukaryotic cells. Nat Commun 10, 194.
Osuna, B.A., Karambelkar, S., Mahendra, C., Christie, K.A., Garcia, B., Davidson, A.R., Kleinstiver, B.P., Kilcher, S., and Bondy-Denomy, J. (2020). Listeria phages induce Cas9 degradation to protect lysogenic genomes. Cell Host Microbe 28, 31–40.e9.
Pawluk, A., Amrani, N., Zhang, Y., Garcia, B., Hidalgo-Reyes, Y., Lee, J., Edraki, A., Shah, M., Sontheimer, E.J., Maxwell, K.L., et al. (2016a). Naturally occurring off-switches for CRISPR-Cas9. Cell 167, 1829–1838.e9.
Pawluk, A., Staals, R.H.J., Taylor, C., Watson, B.N.J., Saha, S., Fineran, P.C., Maxwell, K.L., and Davidson, A.R. (2016b). Inactivation of CRISPR-Cas systems by anti-CRISPR proteins in diverse bacterial species. Nat Microbiol 1, 16085.
Peng, R., Li, Z., Xu, Y., He, S., Peng, Q., Wu, L., Wu, Y., Qi, J., Wang, P., Shi, Y., et al. (2019). Structural insight into multistage inhibition of CRISPR-Cas12a by AcrVA4. Proc Natl Acad Sci USA 116, 18928–18936.
Pinilla-Redondo, R., Shehreen, S., Marino, N.D., Fagerlund, R.D., Brown, C.M., Sørensen, S.J., Fineran, P.C., and Bondy-Denomy, J. (2020). Discovery of multiple anti-CRISPRs highlights anti-defense gene clustering in mobile genetic elements. Nat Commun 11, 5652.
Rauch, B.J., Silvis, M.R., Hultquist, J.F., Waters, C.S., McGregor, M.J., Krogan, N.J., and Bondy-Denomy, J. (2017). Inhibition of CRISPR-Cas9 with bacteriophage proteins. Cell 168, 150–158.e10.
Ren, C., Gathunga, E.K., Li, X., Li, H., Kong, J., Dai, Z., and Liang, Z. (2023). Efficient genome editing in grapevine using CRISPR/LbCas12a system. Mol Horticulture 3, 21.
Ren, Q., Sretenovic, S., Liu, G., Zhong, Z., Wang, J., Huang, L., Tang, X., Guo, Y., Liu, L., Wu, Y., et al. (2021a). Improved plant cytosine base editors with high editing activity, purity, and specificity. Plant Biotechnol J 19, 2052–2068.
Ren, Q., Sretenovic, S., Liu, S., Tang, X., Huang, L., He, Y., Liu, L., Guo, Y., Zhong, Z., Liu, G., et al. (2021b). PAM-less plant genome editing using a CRISPR–SpRY toolbox. Nat Plants 7, 25–33.
Sanz Juste, S., Okamoto, E.M., Nguyen, C., Feng, X., and López Del Amo, V. (2023). Next-generation CRISPR gene-drive systems using Cas12a nuclease. Nat Commun 14, 6388.
Schindele, P., Merker, L., Schreiber, T., Prange, A., Tissier, A., and Puchta, H. (2023). Enhancing gene editing and gene targeting efficiencies in *Arabidopsis thaliana* by using an intron-containing version of ttLbCas12a. Plant Biotechnol J 21, 457–459.
Shin, J., Jiang, F., Liu, J.J., Bray, N.L., Rauch, B.J., Baik, S.H., Nogales, E., Bondy-Denomy, J., Corn, J.E., and Doudna, J.A. (2017). Disabling Cas9 by an anti-CRISPR DNA mimic. Sci Adv 3, e1701620.
Song, G., Tian, C., Li, J., Zhang, F., Peng, Y., Gao, X., and Tian, Y. (2023). Rapid characterization of anti-CRISPR proteins and optogenetically engineered variants using a versatile plasmid interference system. Nucleic Acids Res 51, 12381–12396.
Song, G., Zhang, F., Tian, C., Gao, X., Zhu, X., Fan, D., and Tian, Y. (2022). Discovery of potent and versatile CRISPR–Cas9 inhibitors engineered for chemically controllable genome editing. Nucleic Acids Res 50, 2836–2853.
Song, G., Zhang, F., Zhang, X., Gao, X., Zhu, X., Fan, D., and Tian, Y. (2019). AcrIIA5 inhibits a broad range of Cas9 orthologs by preventing DNA target cleavage. Cell Rep 29, 2579–2589.e4.
Starai, V.J., and Escalante-Semerena, J.C. (2004). Identification of the protein acetyltransferase (Pat) enzyme that acetylates acetyl-CoA synthetase in *Salmonella enterica*. J Mol Biol 340, 1005–1012.
Stewart, C.N., Jr., and Via, L.E. (1993). A rapid CTAB DNA isolation technique useful for RAPD fingerprinting and other PCR applications. Biotechniques 14, 748–750.
Sun, W., Yang, J., Cheng, Z., Amrani, N., Liu, C., Wang, K., Ibraheim, R., Edraki, A., Huang, X., Wang, M., et al. (2019). Structures of *Neisseria meningitidis* Cas9 complexes in catalytically poised and anti-CRISPR-inhibited states. Mol Cell 76, 938–952.e5.
Tang, X., Liu, G., Zhou, J., Ren, Q., You, Q., Tian, L., Xin, X., Zhong, Z., Liu, B., Zheng, X., et al. (2018). A large-scale whole-genome sequencing analysis reveals highly specific genome editing by both Cas9 and Cpf1 (Cas12a) nucleases in rice. Genome Biol 19, 84.
Tang, X., Lowder, L.G., Zhang, T., Malzahn, A.A., Zheng, X., Voytas, D.F., Zhong, Z., Chen, Y., Ren, Q., Li, Q., et al. (2017). Correction: a CRISPR–Cpf1 system for efficient genome editing and transcriptional repression in plants. Nat Plants 3, 17103.
Tang, X., Ren, Q., Yan, X., Zhang, R., Liu, L., Han, Q., Zheng, X., Qi, Y., Song, H., and Zhang, Y. (2024). Boosting genome editing in plants with single transcript unit surrogate reporter systems. Plant Commun 5, 100921.
Tang, X., Ren, Q., Yang, L., Bao, Y., Zhong, Z., He, Y., Liu, S., Qi, C., Liu, B., Wang, Y., et al. (2019). Single transcript unit CRISPR 2.0 systems for robust Cas9 and Cas12a mediated plant genome editing. Plant Biotechnol J 17, 1431–1445.
Tang, X., and Zhang, Y. (2023). Beyond knockouts: fine-tuning regulation of gene expression in plants with CRISPR-Cas-based promoter editing. New Phytol 239, 868–874.
Tang, X., Zheng, X., Qi, Y., Zhang, D., Cheng, Y., Tang, A., Voytas, D.F., and Zhang, Y. (2016). A single transcript CRISPR-Cas9 system for efficient genome editing in plants. Mol Plant 9, 1088–1091.
Thavalingam, A., Cheng, Z., Garcia, B., Huang, X., Shah, M., Sun, W., Wang, M., Harrington, L., Hwang, S., Hidalgo-Reyes, Y., et al. (2019). Inhibition of CRISPR-Cas9 ribonucleoprotein complex assembly by anti-CRISPR AcrIIC2. Nat Commun 10, 2806.
Uribe, R.V., van der Helm, E., Misiakou, M.A., Lee, S.W., Kol, S., and Sommer, M.O.A. (2019). Discovery and characterization of Cas9 inhibitors disseminated across seven bacterial Phyla. Cell Host Microbe 26, 702.
Wang, X., Li, X., Ma, Y., He, J., Liu, X., Yu, G., Yin, H., and Zhang, H. (2022). Inhibition mechanisms of CRISPR-Cas9 by AcrIIA17 and AcrIIA18. Nucleic Acids Res 50, 512–521.
Wang, X., Ye, L., Lyu, M., Ursache, R., Löytynoja, A., and Mähönen, A.P. (2020). An inducible genome editing system for plants. Nat Plants 6, 766–772.
Watters, K.E., Fellmann, C., Bai, H.B., Ren, S.M., and Doudna, J.A. (2018). Systematic discovery of natural CRISPR-Cas12a inhibitors. Science 362, 236–239.
Watters, K.E., Shivram, H., Fellmann, C., Lew, R.J., McMahon, B., and Doudna, J.A. (2020). Potent CRISPR-Cas9 inhibitors from *Staphylococcus* genomes. Proc Natl Acad Sci USA 117, 6531–6539.
Wu, Y., He, Y., Sretenovic, S., Liu, S., Cheng, Y., Han, Y., Liu, G., Bao, Y., Fang, Q., Zheng, X., et al. (2022a). CRISPR-BETS: a base-editing design tool for generating stop codons. Plant Biotechnol J 20, 499–510.
Wu, Y., Ren, Q., Zhong, Z., Liu, G., Han, Y., Bao, Y., Liu, L., Xiang, S., Liu, S., Tang, X., et al. (2022b). Genome-wide analyses of PAM-relaxed Cas9 genome editors reveal substantial off-target effects by ABE8e in rice. Plant Biotechnol J 20, 1670–1682.
Xie, X., Ma, X., Zhu, Q., Zeng, D., Li, G., and Liu, Y.G. (2017). CRISPR-GE: a convenient software toolkit for CRISPR-based genome editing. Mol Plant 10, 1246–1249.
Xu, Q., Liu, Q., Chen, Z., Yue, Y., Liu, Y., Zhao, Y., and Zhou, D.X. (2021). Histone deacetylases control lysine acetylation of ribosomal proteins in rice. Nucleic Acids Res 49, 4613–4628.
Xu, Y., Zhang, L., Ou, S., Wang, R., Wang, Y., Chu, C., and Yao, S. (2020). Natural variations of SLG1 confer high-temperature tolerance in indica rice. Nat Commun 11, 5441.
Xu, Z., Zhang, H., Zhang, X., Jiang, H., Liu, C., Wu, F., Qian, L., Hao, B., Czajkowsky, D.M., Guo, S., et al. (2019). Interplay between the bacterial protein deacetylase CobB and the second messenger c-di-GMP. EMBO J 38, e100948.
Yan, H., Sun, H., Jia, X., Lv, C., Li, J., and Zhao, Q. (2020). Phenotypic, transcriptomic, and metabolomic signatures of root-specifically overexpressed OsCKX2 in rice. Front Plant Sci 11, 575304.
Yang, H., and Patel, D.J. (2017). Inhibition mechanism of an anti-CRISPR suppressor AcrIIA4 targeting SpyCas9. Mol Cell 67, 117–127.e5.
Yang, S., Chang, R., Yang, H., Zhao, T., Hong, Y., Kong, H.E., Sun, X., Qin, Z., Jin, P., Li, S., et al. (2017). CRISPR/Cas9-mediated gene editing ameliorates neurotoxicity in mouse model of Huntington's disease. J Clin Invest 127, 2719–2724.
Yin, C., Zhang, T., Qu, X., Zhang, Y., Putatunda, R., Xiao, X., Li, F., Xiao, W., Zhao, H., Dai, S., et al. (2017). *In vivo* excision of HIV-1 provirus by saCas9 and multiplex single-guide RNAs in animal models. Mol Ther 25, 1168–1186.
You, Q., Zhong, Z., Ren, Q., Hassan, F., Zhang, Y., and Zhang, T. (2018). CRISPRMatch: an automatic calculation and visualization tool for high-throughput CRISPR genome-editing data analysis. Int J Biol Sci 14, 858–862.
Yu, L., and Marchisio, M.A. (2021). *Saccharomyces cerevisiae* synthetic transcriptional networks harnessing dCas12a and type V-A anti-CRISPR proteins. ACS Synth Biol 10, 870–883.
Zetsche, B., Gootenberg, J.S., Abudayyeh, O.O., Slaymaker, I.M., Makarova, K.S., Essletzbichler, P., Volz, S.E., Joung, J., van der Oost, J., Regev, A., et al. (2015). Cpf1 is a single RNA-guided endonuclease of a class 2 CRISPR-Cas system. Cell 163, 759–771.
Zhang, F., Maeder, M.L., Unger-Wallace, E., Hoshaw, J.P., Reyon, D., Christian, M., Li, X., Pierick, C.J., Dobbs, D., Peterson, T., et al. (2010). High frequency targeted mutagenesis in *Arabidopsis thaliana* using zinc finger nucleases. Proc Natl Acad Sci USA 107, 12028–12033.

Zhang, H., Li, Z., Daczkowski, C.M., Gabel, C., Mesecar, A.D., and Chang, L. (2019). Structural basis for the inhibition of CRISPR-Cas12a by anti-CRISPR proteins. Cell Host Microbe 25, 815–826.e4.
Zhang, L., Li, G., Zhang, Y., Cheng, Y., Roberts, N., Glenn, S.E., DeZwaan-McCabe, D., Rube, H.T., Manthey, J., Coleman, G., et al. (2023). Boosting genome editing efficiency in human cells and plants with novel LbCas12a variants. Genome Biol 24, 102.
Zhang, Y., Ren, Q., Tang, X., Liu, S., Malzahn, A.A., Zhou, J., Wang, J., Yin, D., Pan, C., Yuan, M., et al. (2021). Expanding the scope of plant genome engineering with Cas12a orthologs and highly multiplexable editing systems. Nat Commun 12, 1944.
Zheng, X., Zhang, S., Liang, Y., Zhang, R., Liu, L., Qin, P., Zhang, Z., Wang, Y., Zhou, J., Tang, X., et al. (2023). Loss-function mutants of *OsCKX* gene family based on CRISPR-Cas systems revealed their diversified roles in rice. Plant Genome 16, e20283.
Zhong, Z., Liu, G., Tang, Z., Xiang, S., Yang, L., Huang, L., He, Y., Fan, T., Liu, S., Zheng, X., et al. (2023). Efficient plant genome engineering using a probiotic sourced CRISPR-Cas9 system. Nat Commun 14, 6102.
Zhong, Z., Sretenovic, S., Ren, Q., Yang, L., Bao, Y., Qi, C., Yuan, M., He, Y., Liu, S., Liu, X., et al. (2019). Improving plant genome editing with high-fidelity xCas9 and non-canonical PAM-targeting Cas9-NG. Mol Plant 12, 1027–1036.
Zhong, Z., Zhang, Y., You, Q., Tang, X., Ren, Q., Liu, S., Yang, L., Wang, Y., Liu, X., Liu, B., et al. (2018). Plant genome editing using FnCpf1 and LbCpf1 nucleases at redefined and altered PAM sites. Mol Plant 11, 999–1002.
Zhou, J., Deng, K., Cheng, Y., Zhong, Z., Tian, L., Tang, X., Tang, A., Zheng, X., Zhang, T., Qi, Y., et al. (2017). CRISPR-Cas9 based genome editing reveals new insights into microRNA function and regulation in rice. Front Plant Sci 8, 1598.
Zhou, J., Liu, G., Zhao, Y., Zhang, R., Tang, X., Li, L., Jia, X., Guo, Y., Wu, Y., Han, Y., et al. (2023). An efficient CRISPR–Cas12a promoter editing system for crop improvement. Nat Plants 9, 588–604.
Zhou, J., Xin, X., He, Y., Chen, H., Li, Q., Tang, X., Zhong, Z., Deng, K., Zheng, X., Akher, S.A., et al. (2019). Multiplex QTL editing of grain-related genes improves yield in elite rice varieties. Plant Cell Rep 38, 475–485.
Zhou, J., Yuan, M., Zhao, Y., Quan, Q., Yu, D., Yang, H., Tang, X., Xin, X., Cai, G., Qian, Q., et al. (2021). Efficient deletion of multiple circle RNA loci by CRISPR-Cas9 reveals *Os06circ02797* as a putative sponge for *OsMIR408* in rice. Plant Biotechnol J 19, 1240–1252.
Zhou, J., Zhang, R., Jia, X., Tang, X., Guo, Y., Yang, H., Zheng, X., Qian, Q., Qi, Y., and Zhang, Y. (2022). CRISPR-Cas9 mediated *OsMIR168a* knockout reveals its pleiotropy in rice. Plant Biotechnol J 20, 310–322.
Zhu, Y., Gao, A., Zhan, Q., Wang, Y., Feng, H., Liu, S., Gao, G., Serganov, A., and Gao, P. (2019). Diverse mechanisms of CRISPR-Cas9 inhibition by type IIC anti-CRISPR proteins. Mol Cell 74, 296–309.e7.
Zuo, J., Niu, Q.W., and Chua, N.H. (2000). An estrogen receptor-based transactivator XVE mediates highly inducible gene expression in transgenic plants. Plant J 24, 265–273.